

**Preliminary studies on the structural characterization  
of aminoglycoside nucleotidyltransferase ANT(2'')-Ia  
and spectinomycin kinase SpcN**

**Nilufar Sabet-Kassouf**

**Master of Science**

**Department of Biochemistry**

**McGill University**

**Montreal, Quebec**

**A thesis submitted to McGill University in partial  
fulfillment of the requirements of the degree of  
Master of Science**

**August 2013**

**©Copyright by Nilufar Sabet-Kassouf, 2013**

## ABSTRACT

**Aminoglycosides are broad-spectrum antibiotics that corrupt normal protein synthesis by acting on the coding and translocation mechanisms of the 30S ribosomal subunit. The most common mechanism of resistance to this class of antibiotics is enzymatic modification. There are three families of aminoglycoside modifying enzymes: the *N*-acetyltransferases (AAC), the *O*-phosphotransferases (APH), and the *O*-adenyltransferases (ANT). The focus of this thesis is on the APH and ANT families.**

**Spectinomycin kinase (SpcN), also referred to as APH(9)-Ib, catalyzes the phosphorylation of spectinomycin exclusively, rendering it inactive. It shares its substrate specificity with APH(9)-Ia, for which the crystal structure has been described (Fong *et al*, 2010). Structural elements related to substrate binding remain largely conserved within the APH family, and the structural characterization of various APHs can provide valuable insight into structure-function relationships, such as substrate spectrum. Here, we report initial overexpression and purification methods for SpcN and explore solubilization methods to improve protein overexpression.**

**Aminoglycoside nucleotidyltransferase (2'')-Ia (ANT(2'')-Ia) is among the most prevalent and widespread AMEs in North America (Ramirez & Tomalsky, 2010). It catalyzes the transfer of adenosine monophosphate to the 2'' position of 4-6-disubstituted aminoglycosides, preventing binding to the 30S ribosomal subunit. Its clinical relevance makes it an important target for structure-based drug**

**design. Previous studies of ANT(2'')-Ia were limited due to the formation of inclusion bodies during ANT(2'')-Ia overexpression (Ekman *et al.*, 2001). Here, we report the increase in protein solubility and stability as a result of cleaving 50 extraneous amino acids from the N-terminus. Overexpression and purification of this construct yields 17 mg of soluble, stable, and active protein per liter of culture. We used heteronuclear single quantum correlation (HSQC) and HNCACB, CBCAcoNH triple resonance NMR experiments to characterize the protein. We sequentially assigned 144 of the 176 non-proline amide backbone residues of ANT(2'')-Ia. Titration analyses of ANT(2'')-Ia with tobramycin and ATP separately at 1:1 concentration ratios show unique global chemical shift perturbations for each, suggesting different binding pockets for both substrates.**

## **ABRÉGÉ**

**Les aminosides sont une classe d'antibiotiques à large spectre qui affectent l'efficacité de la synthèse protéique. Parmi les mécanismes de résistance contre cette classe d'antibiotique, l'inactivation enzymatique est le plus souvent fréquenté. Il existe trois classes d'enzymes capable d'inactiver les aminosides: les *N*-acetyltransferases (AAC), les *O*-phosphotransferases (APH), et les *O*-adeniltransferases (ANT). Cette thèse discutera les familles ANT et APH.**

**Spectinomycin kinase (SpcN), aussi nommé APH(9)-Ib, catalyse la phosphorylation et l'inactivation de l'aminoside spectinomycin exclusivement. Il partage cette spécificité du substrat avec APH(9)-Ia, pour lequel la structure cristallographique à déjà été caractérisée (Fong *et al.*, 2010). Étant donné que les éléments structurels reliés à la liaison du substrat et au site de reconnaissance sont largement conservés parmi les membres de la famille APH, les études sur la configuration tridimensionnelle des APH fournissent des informations importantes sur la relation entre structure et fonction, dont la spécificité du site de reconnaissance par exemple. Cette thèse explique les démarches prises pour exprimer, solubiliser et purifier SpcN.**

**L'aminoside nucleotidyltransferase 2"-Ia (ANT(2")-Ia) est parmi les enzymes de résistance contre les aminosides les plus souvent fréquentés (Ramirez & Tomalsky, 2010). Il catalyse le transfert de adénosine monophosphate à la position 2" des aminosides 4,6-bisubstitués, ce qui les empêchent de se lier au sous-unité 30S du ribosome. Son importance dans le milieu clinique fait en sorte qu'il est un cible intéressant pour la recherche et le développement**

**d'antibiotiques basée sur les structures tridimensionnelles. À date, les études sur ANT(2'')-Ia ont été limitées par le fait qu'il s'exprime de façon non soluble (Ekman *et al.*, 2001). Nos études, décrivent dans cette thèse, propose une nouvelle forme soluble et active de ANT(2'')-Ia qui serait la version plus physiologiquement exacte. Nous avons pu obtenir 17 mg de protéine pure, soluble et active à partir d'un litre de culture. Nous avons fait l'attribution séquentielle des déplacements chimiques des atomes de la chaîne principale par RMN en utilisant des expériences bi- et tri-dimensionnelles, dont HSQC et HNCACB et CNCAcoNH. Nous avons complété l'attribution de 144 des 176 résidus (excluant les prolines). Nous avons aussi fait des analyses de titration avec les substrats de ANT(2'')-Ia, ATP et tobramicin séparément, à une concentration de 1:1. Ces analyses démontrent des perturbations globales des déplacement chimiques uniques pour chaque interaction, ce qui suggère que les sites de reconnaissances pour chaque substrat sont différents.**

## **ACKNOWLEDGEMENTS**

**I want to thank, first and foremost, my supervisor Dr. Albert Berghuis, for his endless support and encouragement, his incredible patience and invaluable mentorship, and his ability to be a continued source of inspiration and strength. Words cannot express my gratitude.**

**I also want to thank the members of the Berghuis lab who were not only such wonderful people to work with but without whom none of this work would have been possible. A special thank you to Kun Shi for encouraging and guiding me through our exciting project. Thank you to Barry Sleno and Dr. Pedro Romero for help with molecular genetics and sharing their boundless humor. Thank you to Dr. Desire Fong and Jonathan Blanchet for all their help with the SpcN project, and to Dmitri Rodionov, Brahm Yachnin, Dr. Jaeok Park, Shane Caldwell, Miriam Wodrich, Dr. Oliver Baetigg, Dr. David Burk, Michelle Mcevoy, Dr. Stephen Campbell and Tahereh Haji for the great conversations and willingness to help and to answer all my questions.**

**A big thanks to Dr. Guennadi and Dr. Nozhat Safaee for their help with the NMR experiments. I especially want to thank Nozhat Safaee, who was indispensable to this project, for her constant guidance and genuine friendship.**

**Finally, thank you to Hayley Paul, who was an incredible source of love and support for which I will always be grateful.**

# TABLE OF CONTENTS

TABLE OF CONTENTS .....	vi
LIST OF TABLES .....	viii
LIST OF FIGURES.....	ix
LIST OF ABBREVIATIONS.....	xi
<b>1. INTRODUCTION.....</b>	<b>1</b>
<b>1.1 Mechanisms of antibiotic resistance.....</b>	<b>2</b>
<b>1.2 Aminoglycoside antibiotics .....</b>	<b>4</b>
<b>1.2.1 Introduction to aminoglycosides .....</b>	<b>4</b>
<b>1.2.2 Mechanism of aminoglycoside action.....</b>	<b>5</b>
<b>1.2.3 Resistance to aminoglycosides.....</b>	<b>7</b>
<b>1.3 Spectinomycin kinase SpcN.....</b>	<b>13</b>
<b>1.3.1 Background and relationship with APH(9)-Ia.....</b>	<b>13</b>
<b>1.3.2 Mechanism of action .....</b>	<b>13</b>
<b>1.4 Aminoglycoside nucleotidyltransferase (2'')-Ia.....</b>	<b>14</b>
<b>1.4.1 Clinical significance of ANT(2'')-Ia.....</b>	<b>14</b>
<b>1.5 Thesis objectives .....</b>	<b>18</b>
<b>2. MATERIALS AND METHODS .....</b>	<b>19</b>
<b>2.1 Overexpression and purification of SpcN for the purposes of structural studies .....</b>	<b>20</b>
<b>2.1.1 Bacterial Strain and Plasmid .....</b>	<b>20</b>
<b>2.1.2 Sequencing and Mutagenesis .....</b>	<b>20</b>
<b>2.1.3 Overexpression and purification of SpcN<sup>WT</sup> .....</b>	<b>21</b>
<b>2.1.4 Pyruvate Kinase/Lactate Dehydrogenase-Coupled Activity Assay.....</b>	<b>23</b>
<b>2.2 Preliminary structural studies on Aminoglycoside Nucleotidyltransferase (2'')-Ia .....</b>	<b>25</b>
<b>2.2.1 Bacterial Strain and Plasmid .....</b>	<b>25</b>
<b>2.2.2 Sequence Analysis, Mutagenesis and Cloning of ANT(2'')-Ia constructs .....</b>	<b>25</b>
<b>2.2.3 Growth Media and Culture Conditions for overexpression of ANT(2'')-Ia .....</b>	<b>28</b>
<b>2.2.4 Purification of ANT(2'')-Ia<sup>XL</sup> and ANT(2'')-Ia<sup>SC</sup>.....</b>	<b>29</b>
<b>2.2.5 Determination of ANT(2'')-Ia activity by Nucleotidyltransferase Activity Assay.....</b>	<b>33</b>
<b>2.2.6 Nuclear Magnetic Resonance (NMR) studies of ANT(2'')-Ia<sup>SC</sup> .....</b>	<b>35</b>
<b>2.3 Details for analytical methods.....</b>	<b>35</b>
<b>2.3.1 SDS-PAGE .....</b>	<b>35</b>
<b>2.3.2 Agarose gel electrophoresis .....</b>	<b>35</b>
<b>3. RESULTS AND DISCUSSION.....</b>	<b>37</b>
<b>3.1. Spectinomycin Kinase (SpcN).....</b>	<b>38</b>
<b>3.1.1 Sequence Analysis, Cloning and Mutagenesis of SpcN<sup>TAG</sup>.....</b>	<b>38</b>
<b>3.1.2 Purification of SpcN<sup>WT</sup>.....</b>	<b>39</b>
<b>3.1.3 Overexpression and Solubilization of SpcN<sup>WT</sup> .....</b>	<b>41</b>
<b>3.1.4 Pyruvate Kinase/Lactate Dehydrogenase-Coupled Activity Assay.....</b>	<b>44</b>
<b>3.2. Aminoglycoside Nucleotidyltransferase (2'')-Ia.....</b>	<b>46</b>
<b>3.2.1 Refolding Purification of ANT(2'')-Ia<sup>XL</sup>.....</b>	<b>46</b>
<b>3.2.2 Nucleotidyltransferase Activity Assay on ANT(2'')-Ia<sup>XL</sup> .....</b>	<b>48</b>
<b>3.2.3 Sequence Analysis, Cloning and Mutagenesis of ANT(2'')-Ia<sup>XL</sup> .....</b>	<b>51</b>

<b>3.2.4 Overexpression and purification of ANT(2'')-Ia<sup>SC</sup> .....</b>	<b>51</b>
<b>3.2.5 Nucleotidyltransferase Activity Assay on ANT(2'')-Ia<sup>SC</sup> .....</b>	<b>54</b>
<b>3.2.6 Nuclear Magnetic Resonance (NMR) Experiments of ANT(2'')-Ia<sup>SC</sup> ...</b>	<b>55</b>
<b>4. CONCLUSION .....</b>	<b>65</b>
<b>4.1 Conclusion and future directions for SpcN.....</b>	<b>66</b>
<b>4.2 Conclusion and future directions for ANT(2'')-Ia<sup>SC</sup> .....</b>	<b>67</b>
<b>4.3 Final remarks.....</b>	<b>68</b>
<b>References.....</b>	<b>69</b>
<b>Appendix .....</b>	<b>77</b>

## LIST OF TABLES

<b>Table 1-1. Classes and subclasses of aminoglycoside <i>O</i>-phosphotransferases and corresponding resistance profiles.....</b>	<b>10</b>
<b>Table 1-2. Classes and subclasses of aminoglycoside <i>O</i>-adenyltransferases and corresponding resistance profiles.....</b>	<b>12</b>
<b>Table A-1 NMR assignments for ANT(2'')-Ia<sup>SC</sup> .....</b>	<b>77</b>

## LIST OF FIGURES

<b>Figure 1-1. Timeline of the discovery of the major classes of antibiotics. ....</b>	<b>3</b>
<b>Figure 1-2. Aminoglycoside-aminocyclitols are categorized according to their chemical structure. ....</b>	<b>5</b>
<b>Figure 1-3. Schematic of enzymatic inactivation by APH(9)-Ia and SpcN of the streptomycin core containing aminoglycoside spectinomycin. ....</b>	<b>14</b>
<b>Figure 1-4. The proposed reaction scheme of a Theorell-Chance mechanism for an aminoglycoside nucleotidyltransferase reaction catalyzed by ANT(2'')-Ia (represented by "E"). ....</b>	<b>17</b>
<b>Figure 1-5. Structure of kanamycin A and B, differing at position 2' of ring I. ....</b>	<b>17</b>
<b>Figure 2-1 Schematic diagrams of solubility tests done on SpcN<sup>WT</sup> ....</b>	<b>22</b>
<b>Figure 2-2. Determination of SpcN<sup>WT</sup> activity by continuous pyruvate kinase/lactate dehydrogenase-coupled activity assay. ....</b>	<b>24</b>
<b>Figure 2-3. Cloning/expression region for pET-22b(+) (Novagen Cat. No. 69744-3). ...</b>	<b>27</b>
<b>Figure 2-4. Nucleotide and amino acid sequences for ANT(2'')-Ia<sup>XL</sup> and ANT(2'')-Ia<sup>SC</sup>. ...</b>	<b>27</b>
<b>Figure 2-5. Schematic diagram of solubility tests done on ANT(2'')-Ia<sup>XL</sup>. ....</b>	<b>30</b>
<b>Figure 2-6. Standard protocol for ANT(2'')-Ia<sup>XL</sup> overexpression and purification from inclusion bodies. ....</b>	<b>32</b>
<b>Figure 2-7. Determination of ANT(2'')-Ia activity by discontinuous coupled nucleotidyltransferase activity assay. ....</b>	<b>34</b>
<b>Figure 3-1. Analysis by agarose gel electrophoresis of SpcN<sup>WT</sup> mutagenesis product. ...</b>	<b>39</b>
<b>Figure 3-2. SDS-PAGE analysis of SpcN<sup>WT</sup> overexpression in <i>E. coli</i>. ....</b>	<b>40</b>
<b>Figure 3-3. SDS-PAGE analysis of SpcN<sup>WT</sup> following sequential Q-Sepharose and S-Sepharose ion-exchange chromatography. ....</b>	<b>40</b>
<b>Figure 3-4a. Sample SDS-PAGE analysis of SpcN<sup>WT</sup> solubility tests (lysis by sonication). ....</b>	<b>42</b>
<b>Figure 3-4b. Sample SDS-PAGE analysis of SpcN<sup>WT</sup> solubility tests (lysis by BugBuster<sup>®</sup>). ....</b>	<b>43</b>
<b>Figure 3-5. Continuous PK/LDH-coupled activity assay monitoring the decrease in absorbance of NADH upon oxidation. ....</b>	<b>45</b>
<b>Figure 3-6. SDS-PAGE analysis of final product following refolding protocol. ....</b>	<b>47</b>
<b>Figure 3-7. Activity assays for ANT(2'')-Ia<sup>XL</sup> refolded from inclusion bodies. ....</b>	<b>49</b>
<b>Figure 3-8. Sample SDS-PAGE analysis of solubility test on ANT(2'')-Ia<sup>XL</sup>. ....</b>	<b>50</b>
<b>Figure 3-9. Elution profile for the first purification step by nickel affinity chromatography on a Qiagen 5 ml Ni-NTA Superflow Cartridge. ....</b>	<b>52</b>
<b>Figure 3-10. Qualitative analysis by SDS-PAGE of ANT(2'')-Ia<sup>SC</sup> fractions and relative purity after nickel affinity chromatography. ....</b>	<b>52</b>
<b>Figure 3-11. Elution profile for the second purification step by size exclusion chromatography on a Qiagen HiLoad 26/50 Superdex 75 column. ....</b>	<b>53</b>
<b>Figure 3-12. Qualitative analysis by SDS-PAGE of ANT(2'')-Ia<sup>SC</sup> fractions and relative purity after both nickel affinity chromatography and size exclusion chromatography. ....</b>	<b>54</b>
<b>Figure 3-13. Activity assays for ANT(2'')-Ia<sup>SC</sup> following FPLC Ni-NTA and size-exclusion chromatography. ....</b>	<b>55</b>
<b>Figure 3-14 <sup>15</sup>N/<sup>1</sup>H HSQC spectrum of ANT(2'')-Ia<sup>SC</sup> showing sharp peaks and broad chemical shift dispersion. ....</b>	<b>56</b>
<b>Figure 3-15. Assigned HSQC spectrum for ANT(2'')-Ia<sup>SC</sup>. ....</b>	<b>58</b>

**Figure 3-16. Global chemical shift perturbations in  $^{15}\text{N}$ -HSQC spectra of substrate-bound ANT(2'')-Ia<sup>SC</sup> shown by overlapping with the spectrum of apo-ANT(2'')-Ia<sup>SC</sup>.....61**  
**Figure 3-17. Weighted average of the chemical shift perturbations for ANT(2'')-Ia<sup>SC</sup> titrated with tobramycin. ....62**  
**Figure 3-18. Weighted average of the chemical shift perturbations for ANT(2'')-Ia<sup>SC</sup> titrated with ATP. ....63**  
**Figure 3-19. Example of major chemical shift perturbations observed upon substrate binding. ....64**

## LIST OF ABBREVIATIONS

<b>AME</b>	<b>aminoglycoside modifying enzymes</b>
<b>WHO</b>	<b>world health organization</b>
<b>ANT</b>	<b>aminoglycoside nucleotidyltransferase</b>
<b>APH</b>	<b>aminoglycoside phosphotransferase</b>
<b>AAC</b>	<b>aminoglycoside acetyltransferase</b>
<b>ATP</b>	<b>adenosine triphosphate</b>
<b>HSQC</b>	<b>heteronuclear single quantum coherence/correlation</b>
<b>NMR</b>	<b>nuclear magnetic resonance</b>
<b>SpcN</b>	<b>spectinomycin kinase</b>
<b>PK/LDH</b>	<b>pyruvate kinase/lactate dehydrogenase</b>
<b>ANT(2'')-Ia<sup>XL</sup></b>	<b>extra large construct</b>
<b>ANT(2'')-Ia<sup>SC</sup></b>	<b>standard construct</b>
<b>SpcN<sup>WT</sup></b>	<b>wild type</b>
<b>SpcN<sup>TAG</sup></b>	<b>construct encoding N-terminus hexahistidine tag</b>
<b>HGT</b>	<b>horizontal gene transfer</b>
<b>MRSA</b>	<b>methicillin resistant staphylococcus aureus</b>
<b>VRE</b>	<b>vancomycin resistance enterococci</b>
<b>MDR-TB</b>	<b>multi-drug resistant tuberculosis</b>
<b>rRNA</b>	<b>ribosomal ribonucleic acid</b>
<b>DNA</b>	<b>deoxyribonucleic acid</b>
<b>h44</b>	<b>helix 44</b>
<b>A-site</b>	<b>amino-acyl site</b>
<b>tRNA</b>	<b>transfer RNA</b>
<b>GNAT</b>	<b>Gcn5-related N-acetyltransferases</b>
<b>ePK</b>	<b>eukaryotic protein kinase</b>
<b>Acetyl-CoA</b>	<b>acetyl coenzyme A</b>
<b>IPTG</b>	<b>isopropyl <math>\beta</math>-D-1-thiogalactopyranoside</b>

<b>AMP</b>	<b>adenosine monophosphate</b>
<b>E. coli</b>	<b><i>Escherichia coli</i></b>
<b>PCR</b>	<b>polymerase chain reaction</b>
<b>LB</b>	<b>lysogeny broth</b>
<b>OD</b>	<b>optical density</b>
<b>mM</b>	<b>milimolar</b>
<b>μM</b>	<b>micromolar</b>
<b>μm</b>	<b>micrometer</b>
<b>NDSB</b>	<b>non-detergent sulphobetaine</b>
<b>SDS</b>	<b>sodium dodecyl sulfate</b>
<b>C<sub>α</sub></b>	<b>alpha-carbon</b>
<b>C<sub>β</sub></b>	<b>beta-carbon</b>
<b>EDTA</b>	<b>Ethylenediaminetetraacetic acid</b>
<b>DTT</b>	<b>diothiothreitol</b>
<b>g</b>	<b>gravity constant</b>
<b>kDa</b>	<b>kilo Dalton</b>

# **1. INTRODUCTION**

## **1.1 Mechanisms of antibiotic resistance**

The effect of antibiotics was originally referred to as “antibiosis,” which described “one creature destroying the life of another in order to sustain its own...” (Vuillemin, 1889). Alexander Fleming’s discovery of penicillin in 1928 not only concretized the concept of antibiotics, but also launched the medical community into a “golden age” of pharmaceutical research, disease treatment and prevention (Waksman, 1947). The term “antibiotic” replaced “antibiosis” to describe anything “inhibiting the growth or the metabolic activities of bacteria and other micro-organisms by a chemical substance of microbial origin” (Waksman, 1944). Today, the definition is extended to incorporate substances of both microbial and synthetic origins that either kill bacteria or disrupt their growth through inhibition of cell wall synthesis, inhibition of protein synthesis, inhibition of DNA synthesis, competitive inhibition of folic acid synthesis, inhibition of RNA synthesis, or inactivation of key bacterial enzymes (Levy & Marshall, 2004).

Antibiotic resistance is a natural biological process resulting from adaptive evolution. However, the tremendous selective pressure applied by the overuse and misuse of antibiotics in clinical, veterinary and agricultural settings has caused an unprecedented rise in antibiotic resistance and the emergence of multi-drug resistant pathogens (Levy, 1997; Witte, 1998; Mossialos *et al.*, 2010). Some of the most alarming examples are methicillin-resistant *Staphylococcus aureus* (MRSA), multi-drug resistant tuberculosis (MDR-TB), and vancomycin resistant *enterococci* (VRE) (Mossialos *et al.*, 2010). The rapid increase and spread of drug resistance is creating major complications for the treatment and prevention of disease. Today, resistance can be found for each known class of antibiotics (figure 1-1) (van Hoek *et al.*, 2011). Resistance genes are often encoded on mobile genetic elements and are disseminated by horizontal gene transfer through bacterial conjugation, transformation and bacteriophage transmission (Davies & Davies, 2010).

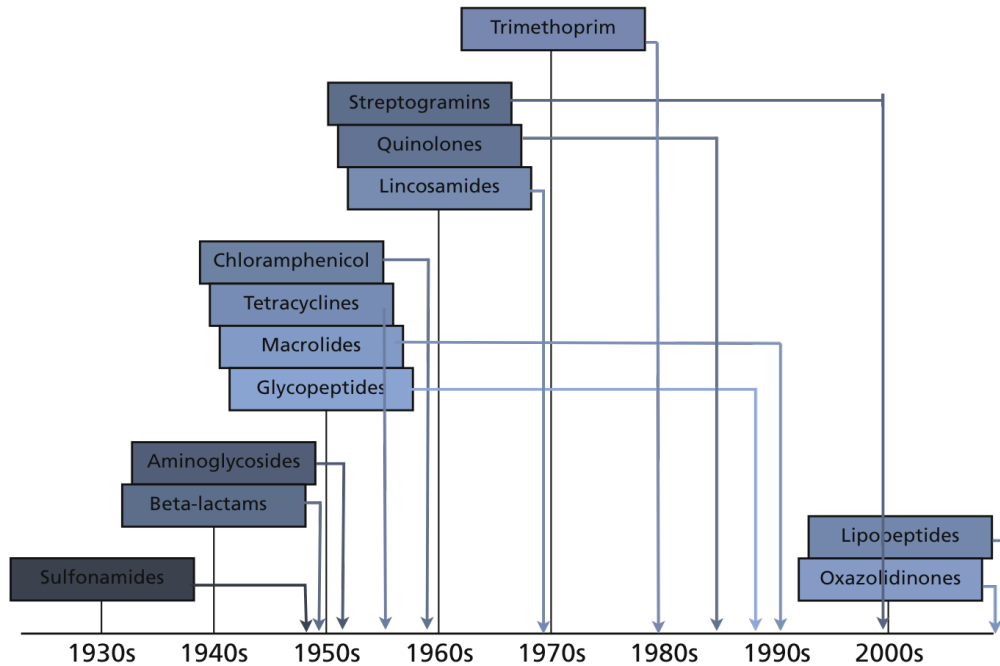


**Figure 1-1. Timeline of the discovery of the major classes of antibiotics.**

Arrows along the timeline respectively illustrate the emergence of resistance to each class.

There are three major mechanisms by which bacteria can be resistant to antibiotics (van Hoek, 2011; Mc Dermott, Walker, & White 2003; Davies & Davies, 2010):

- 1) Decrease of antibiotic concentration in the cell through changes in cell wall permeability, active drug efflux, or drug sequestration;
- 2) Antibiotic inactivation through enzymatic modification or degradation;
- 3) Modification of the target through bypass of metabolic pathways, gene amplification and alteration of the target.

## **1.2 Aminoglycoside antibiotics**

### **1.2.1 Introduction to aminoglycosides**

With the discovery of streptomycin, aminoglycosides were the first effective treatment for tuberculosis, which played a large part in revolutionizing medicine at the beginning of the “golden age” (Schatz, Bugle, & Waksman, 1944; Willis & Arya, 2006). Today, aminoglycosides are known to be powerful broad-spectrum antimicrobials that are most effective against gram-negative bacteria, but are also used in synergy with other antibiotics to target gram-positive bacteria (van Hoek *et al.*, 2011).

Aminoglycosides are part of a family of antibiotics known as the aminoglycoside-aminocyclitols, which are categorized according to their structure. As the name suggests, aminoglycosides in particular are characterized by a central aminocyclitol ring glycosidically linked to amino sugars (figure 1-2). Other members of the aminoglycoside-aminocyclitol family include spectinomycin, which has a streptamine core and does not have an amino sugar, streptomycin, which has a streptidine core, and hygromycin, which has a fused ring system. Most aminoglycosides have a 2-deoxystreptamine central ring, and can be further characterized as being either 4,6-disubstituted or 4,5-disubstituted (figure 1-2) (Busscher, Rutjes, & van Delft, 2004).

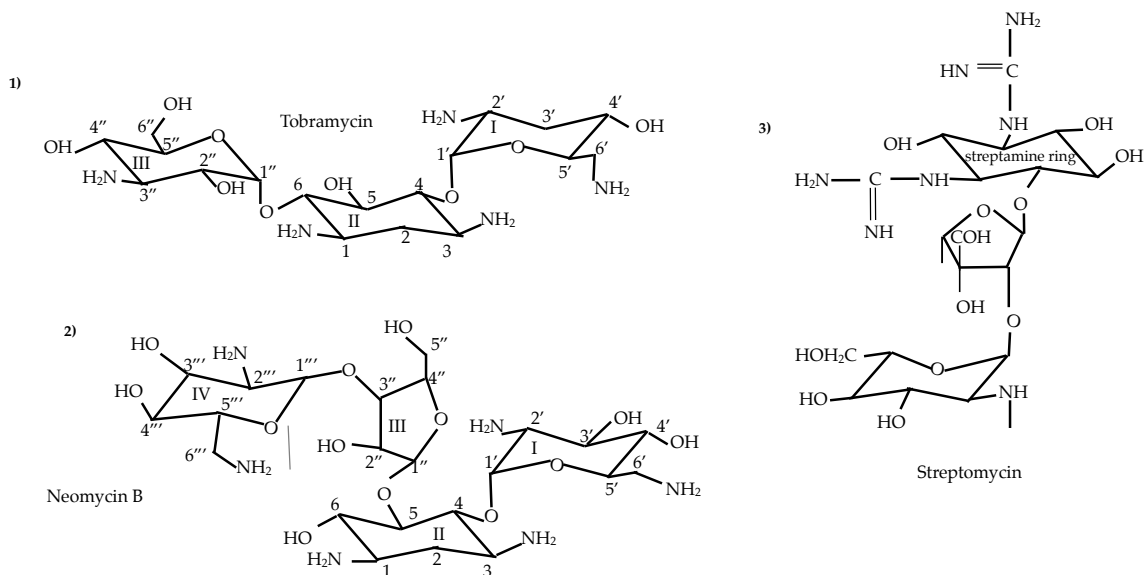


**Figure 1-2. Aminoglycoside-aminocyclitols are categorized according to their chemical structure.**

2-deoxystreptamine aminoglycosides are either a) 4,6-disubstituted or b) 4,5-disubstituted. Streptomycin has a streptidine core and is not linked to an amino sugar (c).

### 1.2.2 Mechanism of aminoglycoside action

Bacterial uptake of aminoglycosides occurs in three main stages: 1) ionic binding of the drug to the cell and hydrophilic diffusion, 2) energy-dependent phase I (EDP-I) and 3) energy-dependent phase II (EDP-II) (Bryan & Van Den Elzen, 1977; Taber *et al.*, 1987). Under biological conditions, aminoglycosides exhibit polycationic properties as a result of their multiple amine groups. They therefore do not readily permeate the cell membrane. Prior to the energy-dependent phases (EDP-I and II), aminoglycosides first bind electrostatically to the outer-membrane triggering the displacement of divalent cations distributed along the cell surface (Hancock *et al.*, 1991; Taber *et al.*, 1987). This allows for limited aminoglycoside entry into the periplasm through hydrophilic diffusion. Energy-dependent aminoglycoside uptake is not yet well understood. EDP-I occurs as a result of the change in membrane potential triggered by the ionic binding phase. This

phase is dependent on the external concentration of aminoglycosides and occurs at a relatively slow rate (Bryan & Van Den Elzen, 1977; Taber *et al.*, 1987). EDP-II, on the other hand occurs at an accelerated rate and appears to be dependent on aminoglycoside binding to the ribosome (Bryan & Van Den Elzen, 1977; Taber *et al.*, 1987).

Once in the cell, the high affinity for nucleic acids resulting from their polycationic nature enables them to bind the 30S ribosomal subunit (Willis & Arya, 2006). Studies have shown that different classes of aminoglycosides bind to the 30S ribosomal subunit at different regions depending on their chemical composition (Kotra, Hadad, & Mobashery, 2000; Recht & Puglisi, 2001).

Aminoglycosides containing a 2-deoxystreptamine ring function by binding the aminoacyl (A-site) at Helix44 (h44). H44 has been shown to have markedly enhanced flexibility, and as such, undergoes major structural deformations in the course of protein synthesis. This is in part attributed to interactions between nucleotides A1492 and A1493 at the base of h44, which are responsible for the fidelity of codon-anticodon pairing during protein translation (Lynch & Puglisi, 2001; Réblová *et al.*, 2006). Binding of 2-deoxystreptamine aminoglycosides triggers the displacement of A1492 and A1493 in a similar manner to that seen with tRNA binding (Tsai *et al.*, 2013). These conformational changes compromise proper translocation and codon-anticodon recognition while the ribosome attempts protein synthesis, decreasing tRNA dissociation rates, interfering with cognate tRNA recognition and resulting in miscoding (Fourmy, Recht, Blanchard, & Puglisi, 1996; Tsai *et al.*, 2013).

Studies on aminoglycosides that contain an aminocyclitol ring other than 2-deoxystreptamine, have shown that they do not displace A1492 and A1493, rather they bind at different regions on the 16S rRNA (Tsai *et al.*, 2013). For example, spectinomycin binds at Helix34 (h34) and hinders proper movement of the ribosome (Carter *et al.*, 2000). These inhibitory effects target protein translocation rather than miscoding and have a bacteriostatic effect rather than bactericidal (Willis & Arya, 2006).

The bactericidal effect of the 2-deoxystreptamine aminoglycosides is mainly attributed to miscoding resulting in the synthesis of aberrant proteins. The proteins then

accumulate in the cell membrane and drastically alter membrane permeability, allowing for increased drug uptake and ribosome saturation (Davis, 1988; Mingeot-Leclercq *et al.*, 1999; Willis & Arya, 2006).

Aminoglycosides have also been shown to interfere with RNA cleavage and the proper functioning of RNase P (Ramirez & Tomalsky, 2010).

### **1.2.3 Resistance to aminoglycosides**

The most prevalent mechanism of resistance to aminoglycosides is the enzymatic modification of hydroxyl and amino groups on the antibiotic that prevent binding to the drug target (Ramirez & Tomalsky, 2010; van Hoek *et al.*, 2011)

There are three major classes of aminoglycoside modifying enzymes (AMEs): 1) the *N*-acetyltransferases (AAC), 2) the *O*-phosphotransferases (APH) and 3) the *O*-adenyltransferases (ANT). AMEs are designated first by a three-letter identifier of their class (AAC, APH or ANT), followed by the site of modification in parenthesis. The specific resistance profile they confer separates them into subclasses that are denoted, immediately after the parenthesis (and hyphen), by a roman numeral. A lower case letter is used as the individual identifier for any specific AME (Shaw *et al.*, 1993). Consider the two enzymes discussed in this thesis: ANT(2'')-Ia, and SpcN, which is also known as APH(9)-Ib, but will be referred to as SpcN in this thesis. ANT(2'')-Ia is an aminoglycoside *O*-adenyltransferase that modifies at position 2'' on the double prime ring (ring III) and would confer a resistance profile corresponding to other ANT(2'')-I modifying enzymes, though none have been found to date. SpcN confers the same resistance profile as APH(9)-Ia, for which a crystal structure has already been described (Fong *et al.*, 2010).

#### **1) Aminoglycoside *N*-acetyltransferases (AAC)**

The aminoglycoside acetyltransferases catalyze the acetyl-CoA-dependent *N*-acetylation of aminoglycosides. The AACs constitute the largest class of AMEs and are

the subject of extensive structural studies. They are divided into four subclasses: AAC(1), AAC(3), AAC(2'), and AAC(6') of which AAC(6')-I constitutes the largest subclass (Ramirez & Tomalsky, 2010). The AACs are members of the GCN5-related *N*-acetyltransferase (GNAT) superfamily. Studies have shown that members of the GNAT superfamily share similar folding motifs that catalyze acetylation by bringing acetyl-CoA in close proximity to the substrate rather than binding to a specific region of the enzyme (Dyda *et al.*, 2000; Wright & Berghuis, 2000).

## **2) Aminoglycoside O-Phosphotransferases (APH)**

APHs catalyze the transfer of the gamma-phosphate from a nucleoside triphosphate to the hydroxyl groups of aminoglycosides (Wright & Thomson, 1999). It is now known that ATP and GTP are used as nucleoside triphosphate substrates for various APHs, (Shakya & Wright, 2010; Shi & Berghuis, 2012). There are currently seven classes of phosphotransferases: APH(4), APH(6), APH(9), APH(3'), APH(2''), APH(3''), and APH(7''). With the exception of the APH(9) and APH(3'') subclasses, the majority of known APH enzymes inactivate aminoglycosides with a 2-deoxystreptamine core (Table 1-1).

The APH(2'') and APH(3') families are the largest, have a wide range of substrate (donor and acceptor) specificity, and together are widely disseminated among Gram-negative and Gram-positive bacteria (Ramirez & Tomalsky, 2010; Vakulenko & Mobashery, 2003). Several crystal structures of members of the APH family have been described to date (Shi *et al.*, 2013). Crystal structures have been described for APH(3')-IIa, APH(3')-IIIa, APH(2'')-IIa, APH(2'')-IIIa, APH(2'')-IVa, all of which have broad substrate specificities for either the donor or the acceptor molecule (Shi *et al.*, 2013). Crystal structures have also been described for APH(4)-Ia and APH(9)-Ia, which have stringent substrate specificities (Shi *et al.*, 2013; Fong *et al.*, 2010).

Crystal structures of APH(3')-IIIa in complex with ADP revealed strong structural homologies centered around the nucleotide-binding pocket of eukaryotic protein kinases (ePK) (Hon *et al.*, 1997). APH(3')-IIIa and APH(2'') (as part of the bifunctional enzyme

AAC(6')-APH(2'')) have been shown to exclusively phosphorylate the serine residues of serine/threonine eukaryotic protein kinases (ePK) substrates (Daigle *et al*, 1998). The structural and functional similarities shared by APHs and ePKs suggest that they share a common ancestor. Though the degree of clinical relevance may vary among different APHs, studies on members of this family offer valuable insight on the mechanisms of substrate binding and specificity, as well as the diversity within the APH family.

<i>O</i> -phosphotransferase enzymes and their subclasses	Aminoglycoside resistance profile	Aminocyclitol core
APH(4) Ia-b	hygromycin	2-deoxystreptamine
APH(6) Ia-d	streptomycin	streptidine
APH(9) Ia-b(SpcN)	spectinomycin	streptamine
APH(3')		
APH(3')-I	kanamycin, neomycin, paromomycin, ribostamycin, lividomycin	2-deoxystreptamine
APH(3')-II	kanamycin, neomycin, butirosin, paromomycin, ribostamycin,	2-deoxystreptamine
APH(3')-IIIa	kanamycin, neomycin, lividomycin, livostamycin, butirosin, amikacin, isepamicin, paromomycin	2-deoxystreptamine
APH(3')-Iva	neomycin, paromycin, ribostamycin	2-deoxystreptamine
APH(2'') Ib-d, IIa, IIIa, IVa	gentamicin	2-deoxystreptamine
APH(3'') Ia-c	streptomycin	streptidine
APH(7'') Ia	hygromycin	2-deoxystreptamine

**Table 1-1. Classes and subclasses of aminoglycoside *O*-phosphotransferases and corresponding resistance profiles.**

### 3) *Aminoglycoside O-Adenyltransferase (ANT)*

ANTs catalyze the ATP-mediated transfer of an AMP onto nucleophilic hydroxyl groups of aminoglycoside substrates. There are five known classes of ANTs: ANT(6), ANT(9), ANT(4'), ANT(2'') and ANT(3''). Though ANT(3'') is the most widely distributed, ANT(4') and ANT(2'') have the highest substrate promiscuity and are also the most clinically relevant (Table 1-2) (Vakulenko & Mobashery, 2003; Ramirez & Tomalsky, 2010).

The only crystal structure reported for the ANTs is that of ANT(4')-Ia (Sakon *et al.*, 1993; Pedersen, Benning, & Holden, 1995). ANT(4')-Ia is also referred to as ANT(4',4'')-Ia because of its ability to modify at the 4'' position of dibekacin, which lacks a 4'-OH. The structure of ANT(4')-Ia in complex with a non-hydrolyzable ATP analogue and kanamycin suggests a potential mechanism for the binding of ANT(4')-Ia substrates (figure 1-1). In this model, aminoglycosides are deprotonated by glutamic acid (most likely Glu145) increasing its nucleophilic properties. ATP interacts with a positive residue such as Lys149, making it more susceptible to direct nucleophilic attack (Wright & Berghuis, 2000). Stereochemical and kinetic analyses on ANT(2'')-I suggest that similar binding takes place through a Theorell-Chance mechanism (Van Pelt, Iyengar, & Frey, 1986; Gates & Northrop, 1988).

While ANTs generally do not show high sequence homology, amino acids lining the substrate binding pockets appear to be conserved (Davies & Wright, 1997). ANT(2'')-Ia shares little sequence homology with other ANTs and even less so with other AMEs (Wright & Serpersu, 2005). It is not uncommon for structural homology to be significant while sequence homology is low. Structural studies on ANT(2'')-Ia can greatly contribute to our knowledge of AME substrate specificity and binding (McKay & Serpersu, 1995). ANT(2'')-Ia is discussed further in section 1.5.

<i>O</i> -adenyltransferases enzymes and their subclasses	Aminoglycoside resistance profile	Aminocyclitol core
ANT(6) Ia-b	streptomycin	streptidine
ANT(9) Ia-b	spectinomycin	streptamine
ANT(4')		
ANT(4')-I	dibekacin, tobramycin, amikacin, isepamicin	2-deoxystreptamine
ANT(4')-IIa-b	tobramycin, amikacin, isepamicin	2-deoxystreptamine
ANT(2'') Ia	gentamicin, tobramycin, dibekacin, sisomicin, kanamycin	2-deoxystreptamine
ANT(3'') Ia	streptomycin spectinomycin	streptidine streptamine

**Table 1-2. Classes and subclasses of aminoglycoside *O*-adenyltransferases and corresponding resistance profiles.**

## **1.3 Spectinomycin kinase SpcN**

### **1.3.1 Background and relationship with APH(9)-Ia**

The APH(9) subclass of aminoglycoside phosphotransferases are the only known APHs capable of inactivating spectinomycin (Ramirez & Tomalsky, 2010). Spectinomycin is among the few aminoglycoside antibiotics that do not have a 2-deoxytreptamine core; rather it has a central streptomine ring (figure 1-3). APH(9)-Ia confers resistance to spectinomycin to *Legionella pneumophila*, the bacterial pathogen responsible for Legionnaires' disease. Interestingly, spectinomycin is not actually used to treat Legionnaires' disease, and therefore exposure to the antibiotic is minimal. Since it is chromosomally encoded and not easily transferable, APH(9)-Ia likely originated as a natural defense mechanism against other spectinomycin-producing organisms (Suter *et al.*, 1997).

SpcN is the only other APH(9) known to date, and it confers the same resistance profile to spectinomycin as APH(9)-Ia (Ramirez & Tomalsky, 2010). It was isolated from *Streptomyces flavopersicus*, which itself produces spectinomycin (Oliver, Goldstein, Bower, Holper, & Otto, 1962). It is not uncommon for genes encoding an antibiotic to be tightly linked to genes encoding resistance and regulatory factors for that antibiotic. As such, SpcN was found to be part of a spectinomycin biosynthesis gene cluster, and studies on this enzyme can offer valuable insight into biosynthetic and evolutionary pathways for AMEs (Lyutzkanova, Distler, & Altenbuchner, 1997). In addition, given that that ANT(3'')-I and ANT(9)-I are the only other AMEs to inactivate spectinomycin, studies on SpcN could also provide insight into common binding mechanisms and protein folding among different AME families (Murphy, 1985; Holligshead & Vapnek, 1985; Ramirez & Tomalsky, 2010).

### **1.3.2 Mechanism of action**

When SpcN was first isolated there was uncertainty about whether it phosphorylated spectinomycin at position 7 or 9 (Figure 1-3) (Lyutzkanova *et al.*, 1997). Phylogenetic analyses revealed that APH(9)-Ia and SpcN cluster closely together, and

since APH(9)-Ia phosphorylates spectinomycin exclusively at position 9, it is likely that SpcN also phosphorylates specifically at position 9 (Wright & Thomson, 1999).

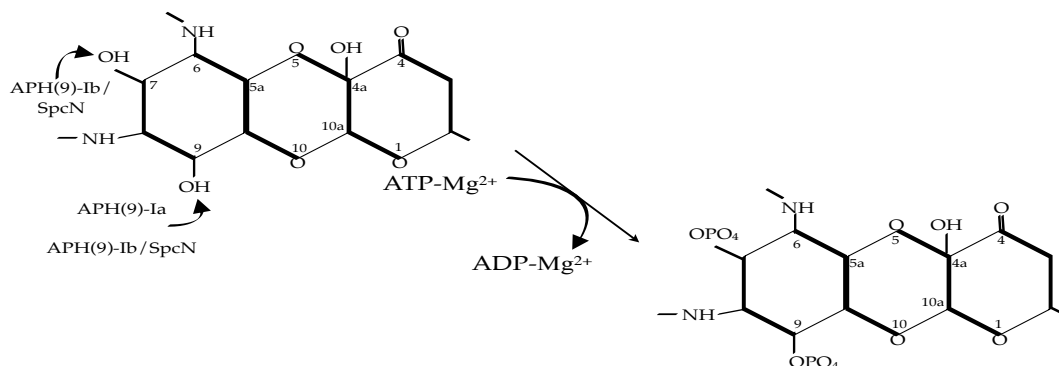


**Figure 1-3. Schematic of enzymatic inactivation by APH(9)-Ia and SpcN of the streptamine core containing aminoglycoside spectinomycin.**

APH(9)-Ia catalyzes the phosphorylation of spectinomycin at position 9. SpcN potentially catalyzes phosphorylation at position 7 or 9.

## 1.4 Aminoglycoside nucleotidyltransferase (2'')-Ia

### 1.4.1 Clinical significance of ANT(2'')-Ia

ANT(2'')-Ia was first identified in 1971 in *Klebsiella pneumonia* as an enzyme encoded by an R-factor mediated resistance gene for gentamicin (Benveniste & Davies, 1971). Since it is commonly encoded by plasmids and transposons, it is the most widely distributed AME of its class, and especially relevant to clinical resistance in Gram-negative bacteria (Vakulenko & Mobashery, 2003). It has been isolated from *Pseudomonas aeruginosa*, *Morganella morganii*, *Escherichia coli*, *Salmonella typhimurium*, *Citrobacter freundii*, and *Acinetobacter baumannii* (Ramirez & Tomalsky, 2010).

Previous work done on ANT(2'')-Ia isolated from an *E. coli* mutant found that the

enzyme is expressed in two forms, likely attributed to two start codons with the same open reading frame. One form is 226 amino acids form with an apparent molecular weight of 29 kDa, and the other is a 249 amino acid form of 35 kDa (Smith & Smith, 1974). Studies on the two forms of the enzyme, cloned from the R-plasmid of a clinical isolate of *Pseudomonas aeruginosa*, have shown that the enzyme expresses as a monomer (Wright & Serpersu, 2004).

ANT(2'')-Ia is frequently associated with bacterial resistance to gentamicin, tobramycin, dibekacin, sisomicin and kanamycin (table 1-1). It has been suggested that the enzyme catalyzes the adenylation of aminoglycosides following an ordered Theorell-Chance mechanism (Figure 1-4) (Gates & Northrop, 1988).

Kinetic studies have shown that enzyme-substrate binding is more favorable for aminoglycosides with 2'-NH<sub>2</sub> (tobramycin, gentamicin, dibekacin, kanamycin B) rather than a 2'-OH (kanamycin A) (Figure 1-5) (Wright & Serpersu, 2005; Wright & Serpersu, 2011). The increased activity seen with a 2'-NH<sub>2</sub> aminoglycoside (compared to 2'-OH) is dependent upon the presence of magnesium as the divalent cation, in contrast to manganese, which results in a 10-fold decrease in enzyme activity (Wright & Serpersu, 2005). Wright and Serpersu have also shown that, in addition to position 2', an amino group and position 1 and 6' are also important determinants of substrate specificity. More generally, rings I and II on 4,6-disubstituted aminoglycosides were shown to be important for substrate specificity in preliminary conformational studies of enzyme-bound aminoglycosides (Ekman, DiGiammarino, Wright, Witter & Serpersu, 2001).

Experiments done to assess the association constant ( $K_b$ ) of various aminoglycosides strongly suggest that binding affinity increases with pH up to approximately 6.8, plateaus at neutral pH and declines at pHs higher than 7.5. These studies showed that neomycin (a competitive inhibitor of ANT(2'')-Ia) and kanamycin display similar binding kinetics at the lower pH range. However at higher pH ranges (>pH8.2), the decrease in affinity for ANT(2'')-Ia is not as drastic for neomycin as it is for the kanamycins. Wright and Serpersu attribute this to the important increases in pKa of amino groups on neomycin upon binding to ANT(2'')-Ia. In fact, increases in pKa of

multiple groups occur on both ligand and enzyme upon binding, and major changes in protonation and deprotonation are widespread across the enzyme's functional groups as well as various substrates (Wright & Serpersu, 2011).

The low stability and solubility of overexpressed ANT(2'')-Ia, and the lack of optimized, functional and simple purification methods have made it very difficult to study (Van Pelt & Northrop, 1984; Wright & Serpersu, 2004). ANT(2'')-Ia, when overexpressed under various conditions, invariably results in over 95% of enzyme being expressed in the form of inclusion bodies (Wright & Serpersu, 2004).

Inclusion bodies are a form of protein aggregation that generally occur either as a disposal mechanism for misfolded proteins or as a bacterial stress response (Villaverde & Carrió, 2003). The formation of inclusion bodies can be the result of many factors involved in protein overexpression. First of all, under normal biological conditions, protein synthesis is most certainly not as high as with genetically engineered recombinant protein synthesis. The increased protein expression can result in an overload of molecular chaperones responsible for proper folding, triggering bacterial stress response mechanisms that utilize inclusion bodies as transient storage systems for eventual protein refolding or proteolysis (Villaverde & Carrió, 2003; Baneyx & Mujacic, 2004). Refolding from inclusion bodies is indeed possible because loss of activity in this form is only moderate (García-Fruitós *et al.*, 2005). The formation of inclusion bodies is inversely correlated to the temperature, IPTG inducer concentrations, and pH of the overexpression media (Sánchez de Groot & Ventura, 2006; Li & Chen, 2009). These parameters are therefore often altered to optimize protein overexpression.

Recently, Serpersu *et al.* optimized a purification protocol based on the refolding of ANT(2'')-Ia from inclusion bodies. The details and implications for this purification will be discussed in later chapters.

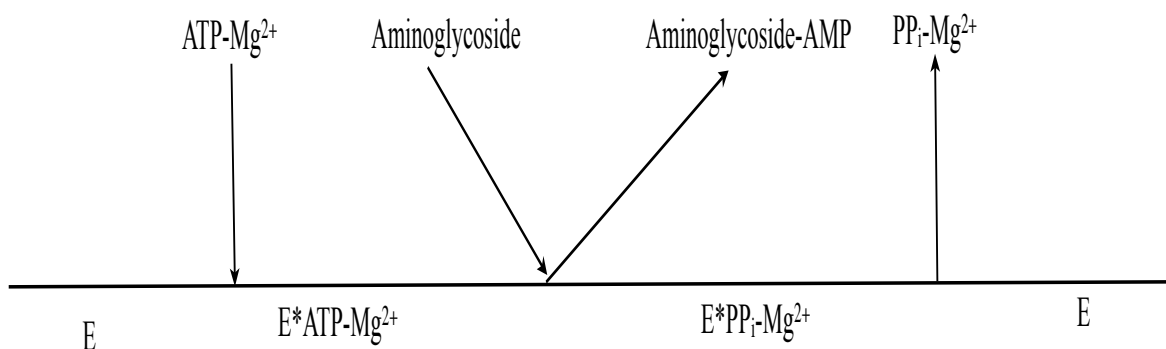


**Figure 1-4. The proposed reaction scheme of a Theorell-Chance mechanism for an aminoglycoside nucleotidyltransferase reaction catalyzed by ANT(2'')-Ia (represented by "E").**

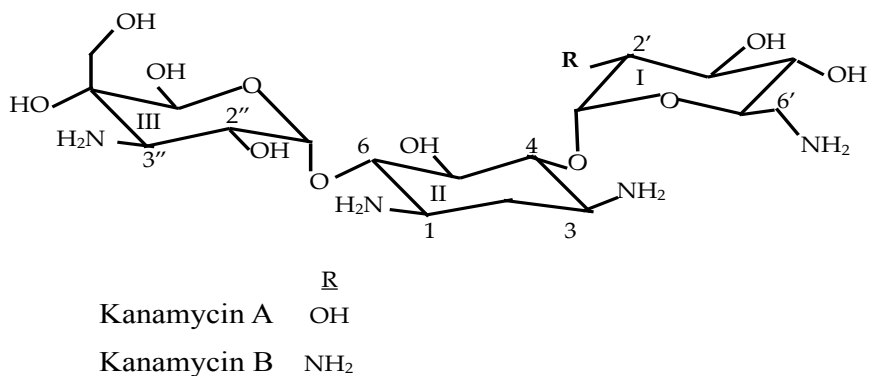


**Figure 1-5. Structure of kanamycin A and B, differing at position 2' of ring I.**

## **1.5 Thesis objectives**

The aim of the research reported in this thesis is to determine the tertiary structures of both SpcN and ANT(2'')-Ia, respectively, in order to gain insight structure-guided inhibition strategies and drug design.

Gaining insight into the structure-function relationship of SpcN can broaden our understanding of the general ANT class, since it is the only other AME class capable of inactivating spectinomycin. Structural studies on SpcN can also shed light on the evolutionary link between protein kinases in a similar way to the tertiary structure of APH(9)-Ia (Fong *et al.*, 2010).

Though a great deal of research has been done into the binding and specificity of ANT(2'')-Ia, structural studies are needed in order to gain a complete insight into mechanisms of action for this enzyme.

## **2. MATERIALS AND METHODS**

Unless otherwise stated, all chemicals used for the following experiments were purchased from Bio-Rad or Sigma Aldrich.

## **2.1 Overexpression and purification of SpcN for the purposes of structural studies**

### **2.1.1 Bacterial Strain and Plasmid**

*SpcN<sup>TAG</sup>* was expressed with an N-terminus 6X-polyhistidine tag and thrombin cleavage site in BL21(DE3) cells transformed with a pET28a(+) expression vector. This construct was prepared in our lab by Jonathan Blanchet and Dr. Desire Fong. *SpcN<sup>WT</sup>* was expressed without any tags in BL21(DE3) cells transformed with a pJOE IPTG inducible plasmid. For both constructs, the gene is inserted between *NdeI* and *HindIII* restriction sites in the multiple cloning region of their respective vectors.

### **2.1.2 Sequencing and Mutagenesis**

Two sets of primers were designed to introduce two mutations in the *SpcN<sup>TAG</sup>* construct: *NdeI* to *NcoI* at the N-terminus, and a silent mutation to an additional *NcoI* site in the gene. Mutagenesis trials were carried out using the Eppendorf Mastercycler<sup>®</sup> Pro and the QuikChange<sup>®</sup> II Site-Directed Mutagenesis Kit. The thermal cycler conditions were as follows: one denaturation cycle of 30 seconds at 95°C, 16 annealing cycles of 30 seconds at 95°C, 2 minute at 55°C, 6 minutes at 68°C. The PCR products digested with Fermentas *NcoI* restriction enzyme were analyzed by agarose gel electrophoresis (see section 2.3.2). To optimize mutagenesis, annealing conditions were modified from 1 minute to 2 minutes at 55°C, or 6 minutes to 13 minutes at 68°C. Optimization techniques from other protocols in literature were also explored (Zheng *et al.*, 2004), Sequencing was carried out by the McGill University and Génome Québec Innovation Centre.

### 2.1.3 Overexpression and purification of SpcN<sup>WT</sup>

To optimize overexpression, the effects of induction temperatures were investigated. A starter culture was prepared by inoculating LB media containing 50 ug/mL ampicillin with *E. coli* BL21(DE3) cells containing pJOE- *SpcN*<sup>WT</sup> from a glycerol culture. Expression cultures were inoculated with starter culture at a 1:50 (v/v) ratio and were induced at an OD<sub>600</sub> of 0.5 with a final IPTG concentration of 0.1 mM. The cultures were incubated at 37°C and 15°C respectively and protein expression was monitored over time using SDS-PAGE analysis (2.3.1).

To optimize SpcN<sup>WT</sup> solubility, we investigated the effects of various expression, induction and lysis parameters. For all solubility tests, soluble and insoluble fractions were separated by centrifugation for 20 minutes at 1700 x g at 4°C and analyzed by SDS-PAGE (section 2.3.1). The following parameters were tested:

- 1) Presence of solubilization agent (figure 2-1a)
- 2) Induction times, temperature, media, and concentration of inducing agent (figure 2-1b)
- 3) Lysis methods. chemical (BugBuster<sup>®</sup> 10X), mechanical (sonication, high pressure homogenization) (figure 2-1b)
- 4) Host cell line. Expression cultures were prepared in ArcticExpress (DE3) competent cells from Agilent Technologies transformed with the *pJOE-SpcN*<sup>WT</sup> vector. The cells were induced with either 0.1 mM IPTG, 0.2 mM IPTG or auto-induction media. All resulting cell pellets were lysed by sonication.

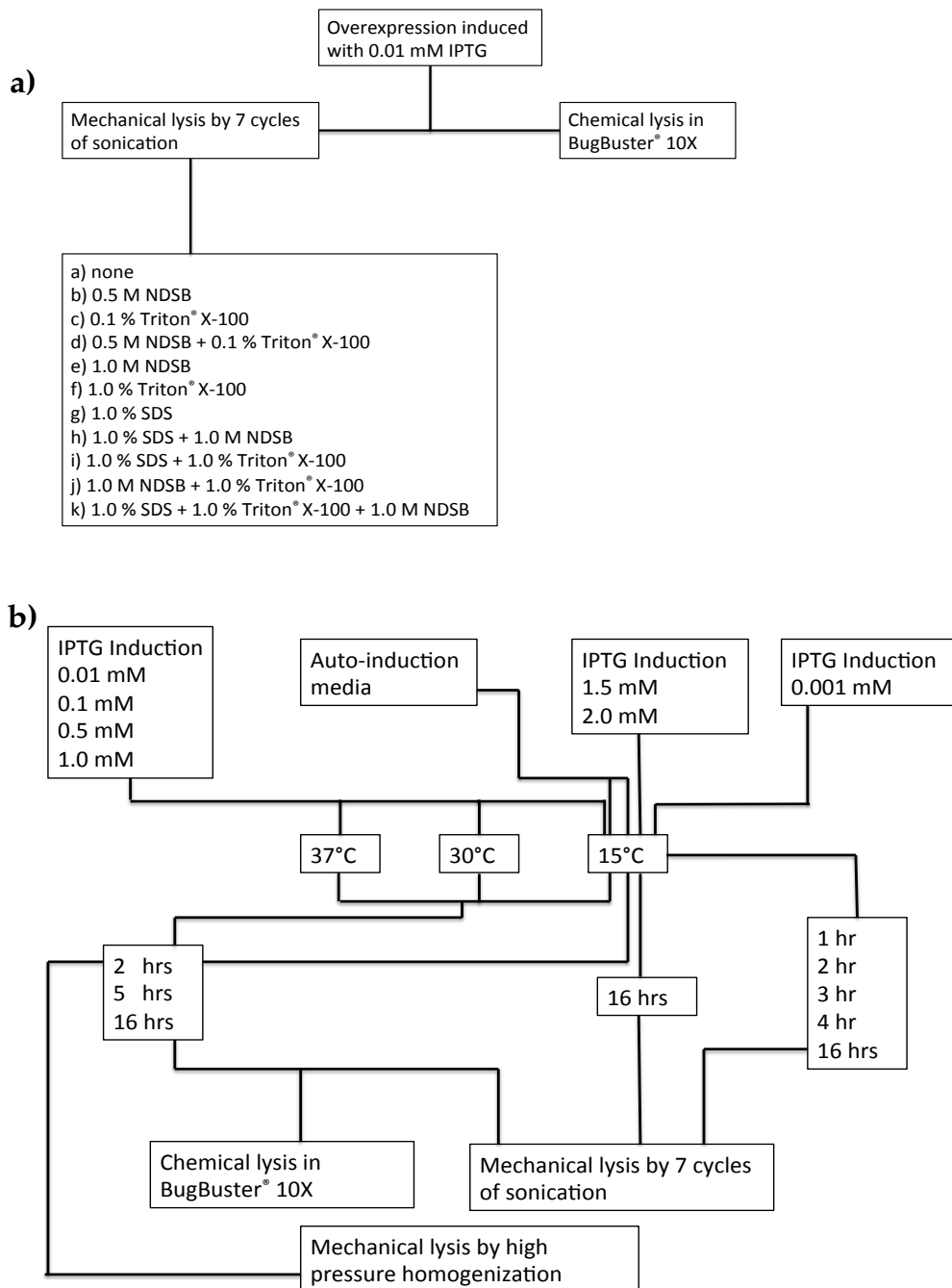


**Figure 2-1 Schematic diagrams of solubility tests done on SpcN<sup>WT</sup>.**

a) Use of solubilizing agents and lysis methods were tested, b) induction media and concentrations, induction temperature, induction time and lysis methods were tested. Mechanical lysis by sonication was done at 7 cycles for 10 seconds. Lysis by high pressure homogenization was done using EmulsiFlex-C3 from Avestin at 15-17000 psi.

### ***Purification of SpcN<sup>WT</sup>***

*SpcN<sup>WT</sup>* was overexpressed in BL21(DE3) cells and induced with 0.1 mM IPTG. Cells were harvested by centrifugation for 15 minutes at 6000 x g at 4°C. The cells were lysed for 15 minutes of 10 seconds cycles in 25 mM Bis-Tris pH 6.0 with one EDTA-free protease inhibitor tablet (complete-mini; Roche). Cell debris was removed by centrifugation for 30 minutes at 50000 x g at 4°C. The supernatant was filtered successively through 0.45  $\mu\text{m}$  and 0.22  $\mu\text{m}$  filters and applied to a HiLoad 16/10 Q Sepharose FF column using the ÄKTA purifier system. The column was equilibrated with 25 mM Bis-Tris pH 6.0 and the protein was eluted with a linear gradient from 0% to 100% of 25 mM Bis-Tris, 2mM NaCl pH 6.0. The purification buffers were selected according to analysis of the titration curve calculated using the Protean<sup>TM</sup> software by the DNASTAR Lasergene® suite. Fractions containing purified SpcN<sup>WT</sup> were pooled and concentrated by centrifugation at 2000 x g and 4°C using Millipore<sup>TM</sup> Amicon<sup>R</sup> Ultra 10K 15ml centrifugal filters.

The concentrated protein sample was applied onto a Mono S HR 515 column using the ÄKTA purifier system. The column was equilibrated with 25 mM AcONa, pH 4.0 and the protein was eluted with a step gradient (0% to 50%, 50%, 50% to 100%) in 25 mM AcONa, 2 M NaCl, pH 4.0. The fractions containing the purified enzyme were once again pooled and the final protein sample was concentrated to 0.41 mg/ml. Purity of SpcN<sup>WT</sup> was qualitatively determined by SDS-PAGE analysis (section 2.3.1).

### **2.1.4 Pyruvate Kinase/Lactate Dehydrogenase-Coupled Activity Assay**

Protein activity was assessed indirectly by monitoring the oxidation of NADH upon release of ADP after the ATP-mediated phosphorylation of spectinomycin by SpcN. The assay is based on the phosphorylation of ADP by pyruvate kinase using phosphoenolpyruvate (PEP), which generates pyruvate. Pyruvate is then converted to lactate by lactate dehydrogenase (LDH) through the oxidation of NADH to NAD<sup>+</sup> (figure

2-2). The reaction was started with the addition of 20 to 40  $\mu$ l concentrated SpcN<sup>WT</sup> (8-41 ug) to a reaction mix of 50 mM Tris, 40 mM KCl, 10 mM MgCl<sub>2</sub>, 0.3 mM NADH, 2.5 mM PEP, 25  $\mu$ lPK/LDH, 1 mM ATP, 0.1 mM spectinomycin. Oxidation of NADH was monitored at 340 nm over 5 minutes.

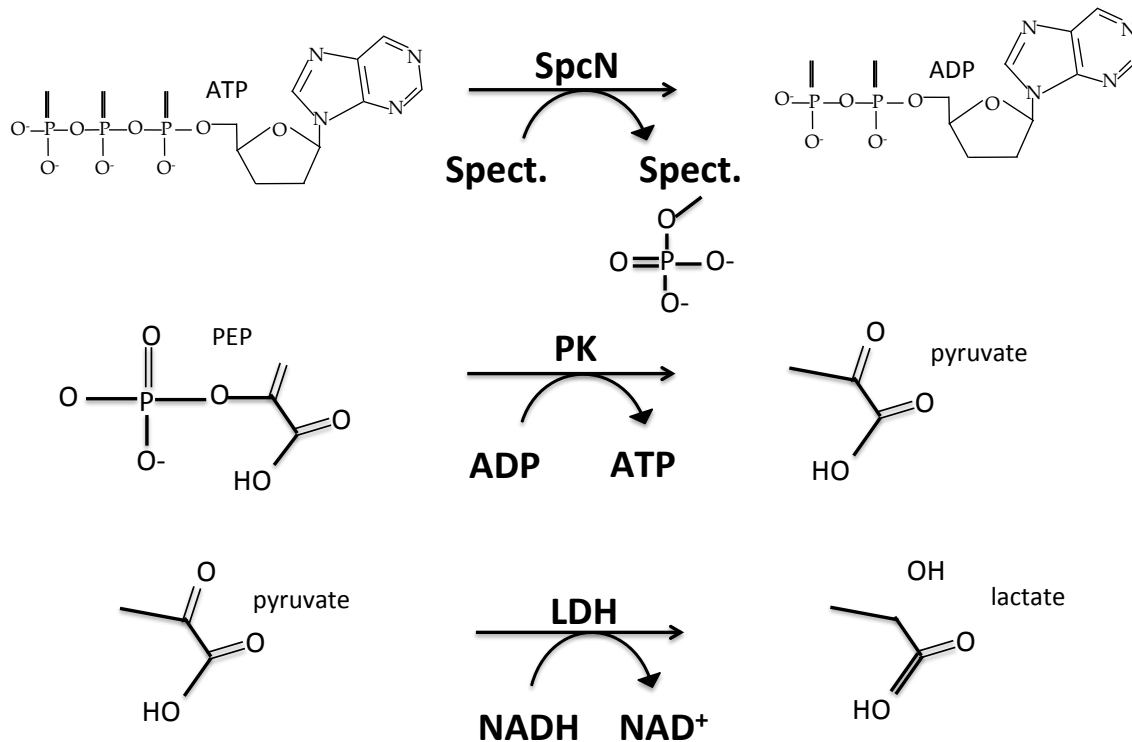


**Figure 2-2. Determination of SpcN<sup>WT</sup> activity by continuous pyruvate kinase/lactate dehydrogenase-coupled activity assay.**

SpcN<sup>WT</sup> catalyzes the ATP-mediated phosphorylation of spectinomycin and releases ADP as a byproduct. The assay indirectly measures SpcN<sup>WT</sup> activity by monitoring the amount of NADH oxidized when LDH catalyzes the conversion of pyruvate to lactate. Pyruvate is generated when PK catalyzes the PEP-mediated phosphorylation of ADP.

## **2.2 Preliminary structural studies on Aminoglycoside Nucleotidyltransferase (2'')-Ia**

Two versions of this enzyme were used throughout the course of these experiments. ANT(2'')-Ia<sup>XL</sup> refers to the version generously provided to us by Dr. Serpersu and ANT(2'')-Ia<sup>SC</sup> refers to the version prepared and cloned in our lab.

### **2.2.1 Bacterial Strain and Plasmid**

In order to carry out structural and functional studies on ANT(2'')-Ia, we sought to overexpress and purify ANT(2'')-Ia<sup>XL</sup>, which we received from Dr. Serpersu's lab at the University of Tennessee. ANT(2'')-Ia<sup>XL</sup> was provided to us in *E. coli* BL21(DE3) cells with the gene inserted between the *Nde*I and *Bam*HI sites in the multiple cloning region of pET-22b(+) (Wright & Serpersu, 2004).

### **2.2.2 Sequence Analysis, Mutagenesis and Cloning of ANT(2'')-Ia constructs**

Before carrying out expression and purification experiments on ANT(2'')-Ia<sup>XL</sup>, it is preferable to analyze the nucleotide sequence and compare it against that reported in literature. To do so, we isolated the plasmid DNA from the BL21(DE3) cells using the protocol from the Qiagen® Plasmid Maxi Kit. The McGill University and Génome Québec Innovation Centre sequenced the resulting plasmid DNA, and sequence alignments were performed using the CLUSTAL 2.0.12 program and the NCBI Basic Local Alignment Search Tool (BLAST).

The ANT(2'')-Ia<sup>XL</sup> construct was mutated to remove the nucleotides coding for amino-acids 1 to 49 of the protein. The original stop codon was replaced by the plasmid encoded polyhistidine tag immediately followed by a new plasmid encoded stop codon (figure 2-1). Mutagenesis was performed using the Eppendorf Mastercycler® Pro. We designed the following oligonucleotides:

Forward oligonucleotide:

5'- AAACATATGGACACAACGCAGGTCACA- 3'

Reverse oligonucleotide:

5'- AAAGCGGCCGCGGCCGCATATCG- 3'

The gene was amplified using the following thermal cycler conditions: 1 cycle of denaturation for 1 minute at 95°C, 25 cycles for annealing for 30 sec at 95°C, 1 minute at 50°C, 3 minutes at 72°C, and 1 cycle of elongation for 10 minutes at 72°C and the reaction was finally held at 4°C indefinitely (QuikChange® Site-Directed Mutagenesis Kit). Gene amplification was confirmed by agarose gel electrophoresis (see section 2.3.2). The PCR product was then purified using the QIAquick® PCR Purification Kit. In order to clone the amplified gene into pET-22b(+), both the vector and the gene were digested overnight at 37°C with *Nde*1 and *Not*1 restriction enzymes. Double-digested pET-22b(+) was purified by agarose gel electrophoresis (sections 2.3.2), and extracted using the QIAquick® Gel Extraction Kit. The *ANT(2'')-Ia<sup>SC</sup>* gene and pET-22b(+) plasmid were ligated overnight at 15°C. *E. coli* DH5α cells were transformed with pET-22b(+)-*ANT(2'')-Ia<sup>SC</sup>* in order to amplify the new plasmid-gene construct. pET-22b(+)-*ANT(2'')-Ia<sup>SC</sup>* was then isolated from a growth culture of *E. coli* using the Qiagen® Plasmid Maxi Kit and used to transform *E. coli* BL21(DE3) cells for protein overexpression.

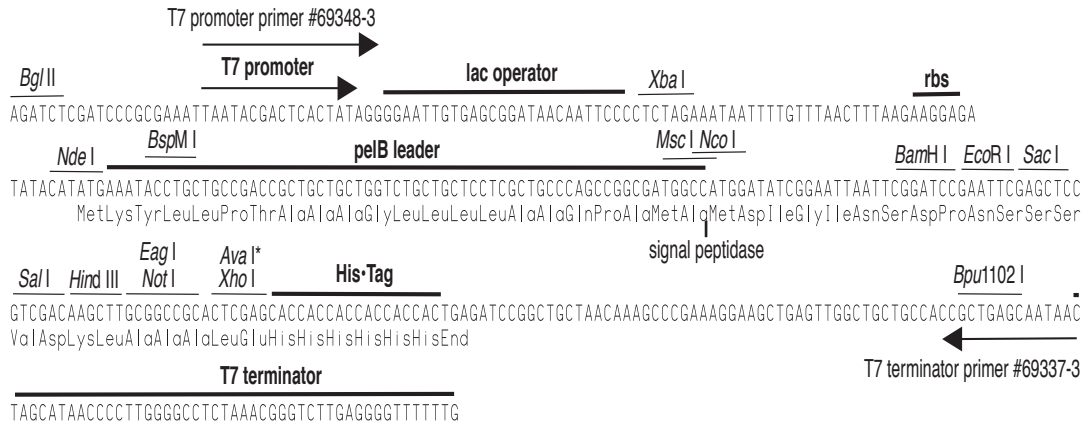


**Figure 2-3. Cloning/expression region for pET-22b(+)** (Novagen Cat. No. 69744-3).

**ANT(2'') - Ia<sup>XL</sup> START**  
 ATGGCTTGTTATGACTGTTTTTTGTACAGTCTATGCCTCGGGCATCCAAGCAGCAAGCGGTTACGCCGTGGGT  
 M A C Y D C F F V Q S M P R A S K Q Q A R Y A V G  
**ANT(2'') - Ia<sup>SC</sup> START**  
 CGATGTTTGATGTTATGGAGCAGCAACGATGTTACGCAGCAGGGCAGTCGCCCTAAAACAAAGTTAGGCCGATG  
 R C L M L W S S N D V T Q Q G S R P K T K L G R M  
 GACACAACGCAGGTACATTGATACACAAAATTCCTAGCTGCGGCAGATGAGCGAAATCTGCCGCTCTGGATCGGT  
 D T T Q V T L I H K I L A A A D E R N L P L W I G  
 GGGGGCTGGGCGATCGATGCACGGCTAGGGCGTGTAACACGCAAGCAGATGATATTGATCTGACGTTTCCCGGC  
 G G W A I D A R L G R V T R K H D D I D L T F P G  
 GAGAGCGCGGCGAGCTCGAGCAATAGTTGAAATGCTCGCGGGCGCGTCATGGAGGAGTTGGACTATGGATTC  
 E R R G E L E A I V E M L G G R V M E E L D Y G F  
 TTAGCGGAGATCGGGGATGAGTACTTACTTACTGCGAACCTGCTTGGTGGGCAGACGAAGCGTATGAAATCGCGGAG  
 L A E I G D E L L D C E P A W W A D E A Y E I A E  
 GCTCCGAGGGCTCGTGCCAGAGGGCGGCTGAGGGCGTATCGCCGGGCGCCAGTCCGTTGTAACAGCTGGGAG  
 A P Q G S C P E A A E G V I A G R P V R C N S W E  
 GCGATCATCTGGGATTACTTTTACTATGCCGATGAAGTACCACCAGTGGACTGGCCTACAAAGCACATAGAGTCC  
 A I I W D Y F Y Y A D E V P P V D W P T K H I E S  
 TACAGGCTCGCATGCACCTCACTCGGGCGGAAAAGTTGAGGTCTTGCGTGCCGCTTTCAGGTCCCAGATATGCC  
 Y R L A C T S L G A E K V E V L R A A F R S R Y A  
**ANT(2'') - Ia<sup>XL</sup> END** **ANT(2'') - Ia<sup>SC</sup> END**  
 GCCTAACTCGAGCACCACCACCACCACCACTGA  
 A \* L E H H H H H H \*

**Figure 2-4. Nucleotide and amino acid sequences for ANT(2'')-Ia<sup>XL</sup> and ANT(2'')-Ia<sup>SC</sup>.**

The start site for ANT(2'')-Ia<sup>SC</sup> is found 50 amino acids downstream of the start site for the ANT(2'')-Ia<sup>XL</sup> open reading frame.

### **2.2.3 Growth Media and Culture Conditions for overexpression of ANT(2'')-Ia**

In order to purify ANT(2'')-Ia<sup>XL</sup> and ANT(2'')-Ia<sup>SC</sup>, BL21(DE3) cells were cultured in nutritional media and enzyme overexpression was induced with IPTG. To assess optimal protein overexpression, the cells were cultured and expression was induced using two different methods. The cells were either cultured in lysogeny broth (LB) nutritional media with direct IPTG induction, or they were cultured in auto-inducing media, which uses a mixture of glucose, glycerol and lactose, where the lactose gradually induced protein expression once it is used as a carbon source.

Overexpression in LB media was performed as follows. A starter culture was prepared by inoculating LB media containing 50 ug/mL ampicillin with *E. coli* BL21(DE3) cells containing plasmid pET-22b(+)-ANT(2'')-Ia<sup>XL or SC</sup> from a glycerol culture. Large-scale growth was performed by inoculating 1 L of LB with starter culture at a 1:50 (v/v) ratio. Protein overexpression was induced at an OD<sub>600</sub> of 0.5 with a final IPTG concentration of 0.1 mM. Unless otherwise stated, induction was carried out for 2.5 hours at 37°C and transferred to 15°C for 16 hours.

Overexpression in auto-inducing media was adapted from an established auto-induction protocol and was performed as follows (Studier, 2005). A starter culture was once again prepared by inoculating LB media containing 50 ug/mL ampicillin with *E. coli* BL21(DE3) cells containing plasmid pET-22b(+)-ANT(2'')-Ia<sup>XL or SC</sup> from a glycerol culture. Large-scale growth was performed by inoculating 1 L of auto-induction media with starter culture at a 1:100 (v/v) ratio. Auto-induction was carried out for 2.5 hours at 37°C and transferred to 15°C for 16 hours. The auto-induction medium is a ZYP-5052 broth consisting of 10 g/L Tryptone, 5 g/L yeast extract, a final concentrations of 1 mM MgSO<sub>4</sub>, 1X NPS salt solution ((NH<sub>4</sub>)<sub>2</sub>SO<sub>4</sub>, KH<sub>2</sub>PO<sub>4</sub>, Na<sub>2</sub>HPO<sub>4</sub>), and a 1X 5052 sugar solution (0.5% glycerol, 0.05% glucose, 0.2% α-lactose).

An additional culture medium was used exclusively when overexpressing ANT(2'')-Ia<sup>SC</sup> for the purposed of NMR studies. In this case, overexpression in M9 minimal media

(0.04 mM Na<sub>2</sub>HPO<sub>4</sub>, 0.02 mM KH<sub>2</sub>PO<sub>4</sub>, 0.09 mM NaCl salt solution, 1.0 M MgSO<sub>4</sub>, 100 mM CaCl<sub>2</sub>, 0.0001 % thiamine, 10 mM FeSO<sub>4</sub>, 0.01% ampicillin, 0.2 % glucose and 0.05 % NH<sub>4</sub>Cl)<sup>1</sup> was carried out as follows. A starter culture was prepared by inoculating LB media containing 50 ug/mL ampicillin with *E. coli* BL21(DE3) cells containing plasmid pET-22b(+)-ANT(2'')-Ia<sup>SC</sup> from a glycerol culture. The starter culture was incubated for 6-8 hours at 37°C. A new starter culture was then prepared by inoculating M9 minimal media containing 50 ug/mL ampicillin with cells from the LB starter culture at 1:50 (v/v) ratio. This new starter culture was incubated for 16 hours at 37°C. After 16 hours, large-scale growth was performed by inoculating 1 L of M9 minimal media at 1:50 (v/v) ratio. Protein overexpression was induced at an OD<sub>600</sub> of 1.0 with a final IPTG concentration of 0.1 mM. Induction was carried out for 2.5 hours at 37°C and transferred to 15°C for 16 hours.

## **2.2.4 Purification of ANT(2'')-Ia<sup>XL</sup> and ANT(2'')-Ia<sup>SC</sup>**

### **2.2.4.1 Purification of ANT(2'')-Ia<sup>XL</sup>**

To optimize ANT(2'')-Ia<sup>XL</sup> overexpression, induction parameters for IPTG concentration, induction time and temperature were investigated. Cell cultures were induced with varying final concentrations of IPTG: 0.05 mM, 0.1 mM, 0.5 mM, and 1.0 mM. For each IPTG concentration, induction times of 1 to 16 hrs and induction temperatures of 37°C, 30°C and 15°C were tested.

To improve ANT(2'')-Ia<sup>XL</sup> solubility, we investigated the effects of induction parameters, host cell, lysis methods and presence of a solubilizing agent (figure 2-3). Samples for each were harvested by centrifugation at 8000 rpm for 3 minutes and the resulting pellets were resuspended in buffer (50 mM Tris-HCl pH 7.5, 10% glycerol).

---

<sup>1</sup> Depending on the spectrum required (HSQC, CBCAcoNH, HNCACB), ammonium chloride and glucoside were replaced with their isotopically labeled counterparts; ammonium-15N chloride and D-Glucose-13C<sub>6</sub>, which we purchased from ISOTECH® at Sigma-Aldrich.

All samples were analyzed by SDS-PAGE (Section 2.3.1).

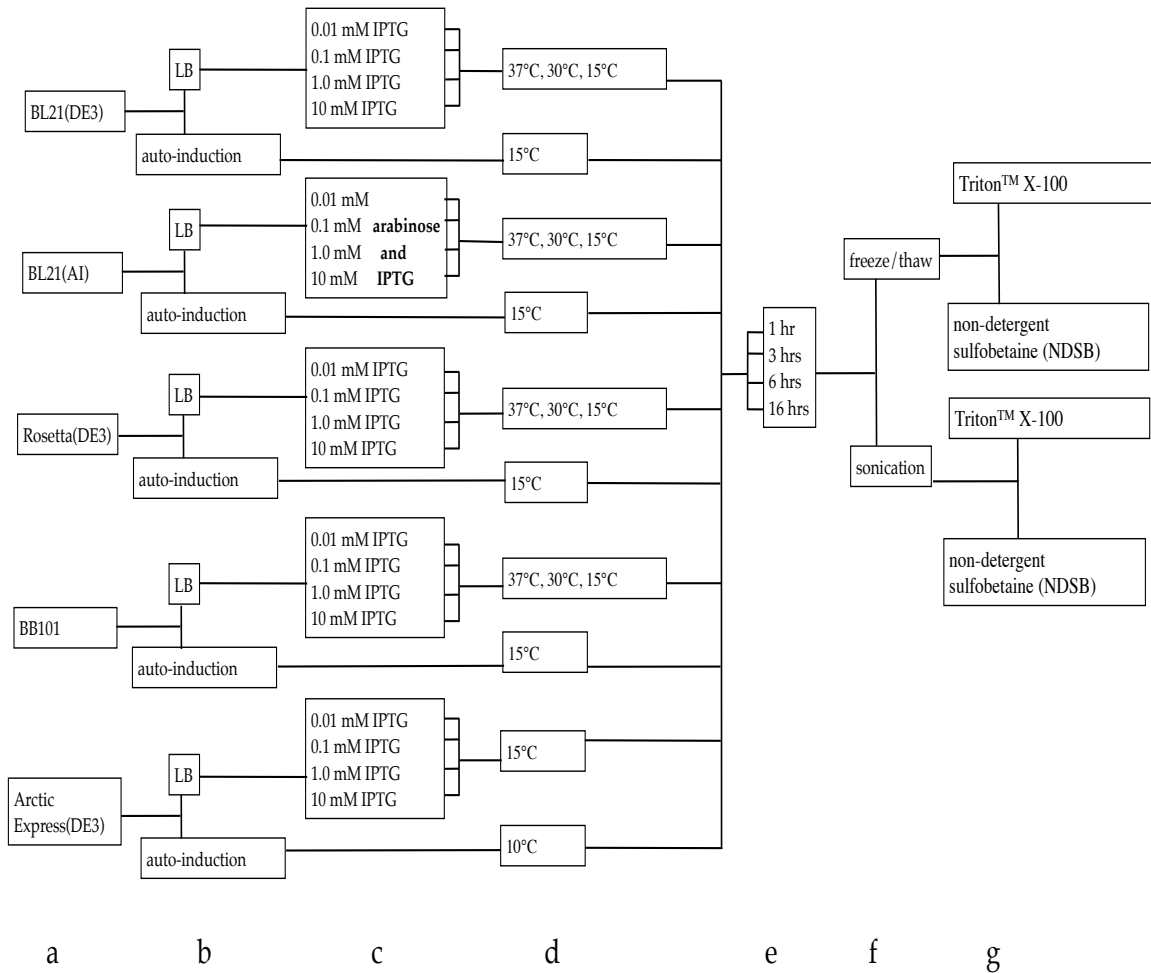


**Figure 2-5. Schematic diagram of solubility tests done on ANT(2'')-Ia<sup>XL</sup>.**

Seven parameters were investigated: **a)** host cell line; **b)** induction media; **c)** concentration of inducing agent; **d)** induction temperatures; **e)** induction time; **f)** lysis method; **g)** use of solubilizing agent.

In order to purify ANT(2'')-Ia<sup>XL</sup> for the purposes of structural studies, we adapted the protocol for purifying ANT(2'')-Ia from inclusion bodies as outlined by Serpersu *et al.* (Wright & Serpersu, 2004).

Protein expression was induced using 0.5 mM IPTG for 3. The cells were harvested by centrifugation at 5000 x g for 30 minutes. The pellets were washed in Buffer A (10 mM Tris-HCl pH 8.0, 0.1 M NaCl, 1 mM EDTA) and centrifuged again at 6000 x g for 15 minutes at 4°C. Cells were lysed in Buffer A by sonication for 15 minutes of 10-second cycles. The lysates were centrifuged at 12000 x g for 15 minutes at 4°C. The supernatants were discarded and the pellets were each washed twice in 10 mM Tris-HCl pH 8.0, 1 mM EDTA, 10 mM DTT, 0.5% (v/v) Triton<sup>TM</sup> X-100 and twice again in 10 mM Tris-HCl pH 8.0, 1 mM EDTA, 10 mM DTT. Samples were centrifuged at 20000 x g for 20 minutes at 4°C after each washing step. The pellets from the final centrifugation were each solubilized in 8 M urea, 0.1 M Tris-HCl pH 8.0, 10 mM DTT, and incubated at room temperature for 1-2 hrs. The samples were centrifuged for 30 minutes at 30000 x g at 4°C to remove the non-soluble components. Refolding of ANT(2'')-Ia<sup>XL</sup> was done at 1:1 ratios (v/v) of solubilized inclusions bodies and refolding buffer (100 mM Tris-HCl pH 8.5, 200 mM KCl, 400 mM L-arginine, and 5 mM reduced glutathione), and incubated overnight at 4°C. The protein was concentrated at 4°C using Millipore<sup>TM</sup> Amicon<sup>R</sup> Ultra 10K centrifugal filters. An overall yield of 72.5 mg of pure ANT(2'')-Ia<sup>XL</sup> was obtained from 1L of culture.

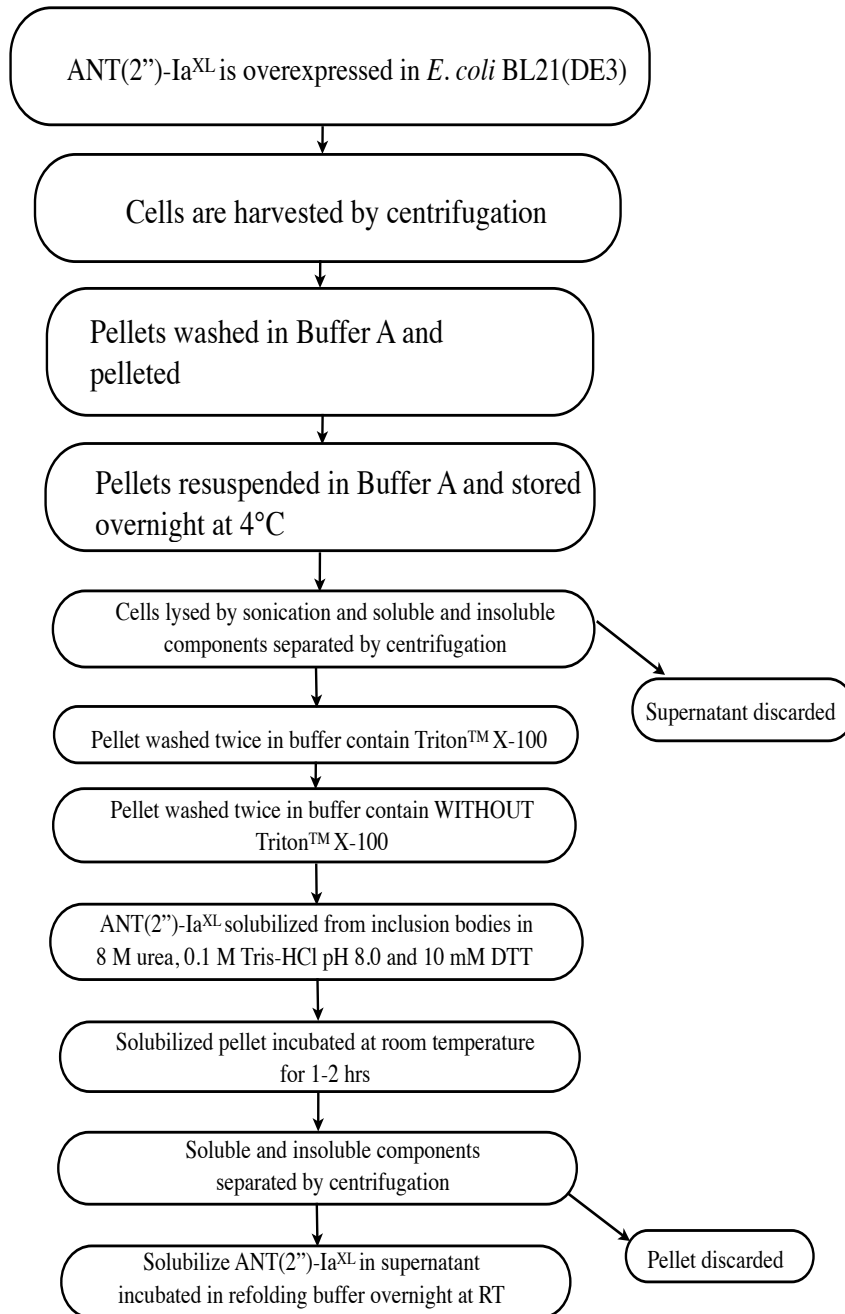


**Figure 2-6. Standard protocol for ANT(2'')-Ia<sup>XL</sup> overexpression and purification from inclusion bodies.**

#### **2.2.4.2 Purification of ANT(2'')-Ia<sup>SC</sup>**

ANT(2'')-Ia<sup>SC</sup> was overexpressed as described in section 2.1.3. Cells were harvested by centrifugation at 6000 x g for 15 min. The cells were lysed by 20 minutes of 10-second cycles of sonication in 50 mM Tris-HCl, pH 8.0<sup>2</sup>, 200 mM NaCl, with 1 EDTA-free protease inhibitor tablet (complete-mini; Roche). Cell debris was removed by centrifugation at 50000 x g for 30 min at 4°C. The supernatant was filtered successively through 0.45 μm and 0.22 μm filters and applied to a Qiagen 5 ml Ni-NTA Superflow Cartridge column using the ÄKTA purifier system. The column was equilibrated with buffer A (50 mM Tris-HCl pH 8.0, 200 mM NaCl and 10 mM imidazole). ANT(2'')-Ia<sup>SC</sup> was eluted with either a linear gradient of buffer A to (0-100%) buffer B (50 mM Tris-HCl pH 8.0, 200 mM NaCl and 500 mM imidazole) or a step was gradient (0%, 2%, 10%, 30%, 100% buffer B). Fractions containing ANT(2'')-Ia<sup>SC</sup> were concentrated centrifugation at 4°C using Millipore<sup>TM</sup> Amicon<sup>R</sup> Ultra 10K centrifugal filters.

The concentrated protein sample was applied to a Qiagen HiLoad 26/50 Superdex 75 column using the ÄKTA purifier and was eluted in 50 mM Tris-HCl, pH 8.0, 200 mM NaCl<sup>3</sup>. The final protein sample was pooled and concentrated by Millipore centrifugal filters as described earlier. Purified ANT(2'')-Ia<sup>SC</sup> concentrated to 11 mg/ml, was analyzed by SDS-PAGE (section 2.3.1), stored at both -80 and 4°C, and used for subsequent analysis by nucleotidyltransferase activity assay, and NMR studies.

#### **2.2.5 Determination of ANT(2'')-Ia activity by Nucleotidyltransferase Activity Assay**

To determine whether the enzyme retained activity throughout purification, we followed the protocol for a nucleotidyltransferase activity assay outlined for ANT(2'')-Ia (Serpersu *et al.*, 2008). ANT(2'')-Ia catalyzes the transfer of AMP from ATP onto aminoglycosides, resulting in the release of inorganic pyrophosphate and modified

---

<sup>2</sup> pH of buffers was lowered to 7.0 when purifying ANT(2'')-Ia<sup>SC</sup> for NMR studies.

<sup>3</sup> Concentration of NaCl was lowered to 50 mM when purifying ANT(2'')-Ia<sup>SC</sup> for NMR studies.

aminoglycoside. This discontinuous coupled enzyme assay spectrophotometrically measures the release of two molecules of inorganic phosphate that occurs when pyrophosphatase hydrolyzes the reaction product of ANT(2'')-Ia, inorganic pyrophosphate (figure 2-5).

We added 25  $\mu$ l of 0.5 to 0.1 mg/ml of purified enzyme to an assay mix consisting of 0.25 M HEPES pH 7.5, 1.0 M KCl, 100 mM MgCl<sub>2</sub>, 20 mM ATP and 2.0 units of inorganic pyrophosphatase. The reaction mix is equilibrated to 30°C and the reaction is started by the addition of 2.5 mM tobramycin. The reaction was then stopped every two minutes with a 1:1 mixture of 1% ammonium molybdate and 10% ascorbic acid. The amount of inorganic phosphate that was released was measured by spectrophotometry at 820 nm. The same assay was used to measure the steady-state rate of reaction catalyzed by both ANT(2'')-Ia<sup>XL</sup> and ANT(2)-Ia<sup>SC</sup>.

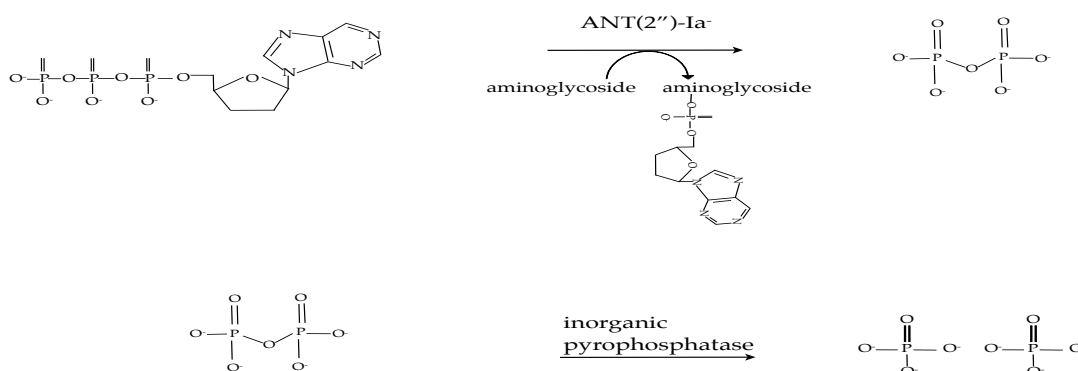


**Figure 2-7. Determination of ANT(2'')-Ia activity by discontinuous coupled nucleotidyltransferase activity assay.**

ANT(2'')-Ia catalyzes the ATP-mediated adenylation of the 2''-OH group of aminoglycosides and releases inorganic pyrophosphate as a byproduct. The assay indirectly measures ANT(2'')-Ia activity by monitoring the amount of inorganic phosphate released upon hydrolysis of inorganic pyrophosphate by inorganic pyrophosphatase.

## **2.2.6 Nuclear Magnetic Resonance (NMR) studies of ANT(2'')-Ia<sup>SC</sup>**

Data for heteronuclear single quantum correlation (HSQC) and triple resonance (HNCACB, CBCAcoNH) experiments on 0.7 mM ANT(2'')-Ia<sup>SC</sup> in NMR buffer (50 mM Tris-HCl, pH 7.0, 50 mM NaCl) were collected at 30°C on a high-sensitivity cold probe using a 600 MHz Bruker spectrometer. HSQC titration experiments were performed on 0.5 mM ANT(2'')-Ia<sup>SC</sup> in NMR buffer with tobramycin and ATP at varying protein to ligand concentration ratios (1:1, 1:2, 1:2:2). HSQC spectra recorded at increasing temperatures (25°C, 30°C, 35°C, 40°C, 45°C, 50°C) were monitored for changes in signal resolution for 0.2 mM ANT(2'')-Ia<sup>SC</sup> in NMR buffer. All data were processed using NMRPipe and spectra were analyzed using Sparky (Delaglio *et al.*, 1995; Goddard & Kneller, SPARKY 3).

## **2.3 Details for analytical methods**

### **2.3.1 SDS-PAGE**

Samples were prepared in 2X SDS-PAGE loading buffer and were heated at 95°C for 5 minutes before being loaded onto 12% polyacrylamide gels. The gels were run at 150-200 V. Proteins were stained with Coomassie® Blue Staining (Invitrogen).

### **2.3.2 Agarose gel electrophoresis**

Samples were prepared in 6X loading dye. A 1% agarose gel was prepared using 1:1 (v/v) ratio of 1X TAE and agarose. The DNA was visualized with ethidium bromide under UV light. Gels were run from 80V to 150V.



### **3. RESULTS AND DISCUSSION**

### **3.1. Spectinomycin Kinase (SpcN)**

#### **3.1.1 Sequence Analysis, Cloning and Mutagenesis of *SpcN*<sup>TAG</sup>**

SpcN is a 329 amino acid protein with a molecular weight of 35.9 kDa and an extinction coefficient of 47,565 M<sup>-1</sup>cm<sup>-1</sup>.

Crystallization trials previously performed in our lab using 10 mg/ml N-terminal his-tagged SpcN<sup>TAG</sup> consistently resulted in precipitation. Attempts to cleave the hexahistidine tag following purification resulted in partial or no cleavage, suggesting that the hexahistidine tag may be inaccessible when placed at the N-terminus (Jonathan Blanchet, Berghuis lab, personal communication). To determine the effects of the placement of a hexahistidine tag on thrombin cleavage and crystallization, we attempted to clone an *SpcN*<sup>TAG</sup> construct with the affinity tag at the C-terminus rather than the N-terminus. Two site-directed mutations were designed to change the restriction enzymes flanking the gene:

- 1) Histidine to proline; *NdeI* (CATATG) to *NcoI* (CCATGG).
- 2) Silent mutation of an additional *NcoI* cut site further downstream within the gene; (CCATGG to CTATGG).

Qualitative analysis of mutagenesis by agarose gel electrophoresis shows that no gene amplification is taking place. Rather primer-dimer formation is consistently observed. Common strategies to overcome primer-dimer formation include optimization of primer design, amplification reaction components, amplification enzyme, and cycling conditions. Modification of cycling conditions, and amplification reaction components did not improve mutagenesis and primer-dimers continued to form, suggesting that further optimization of PCR conditions is needed (figure 3-1) (section 2.1.2).

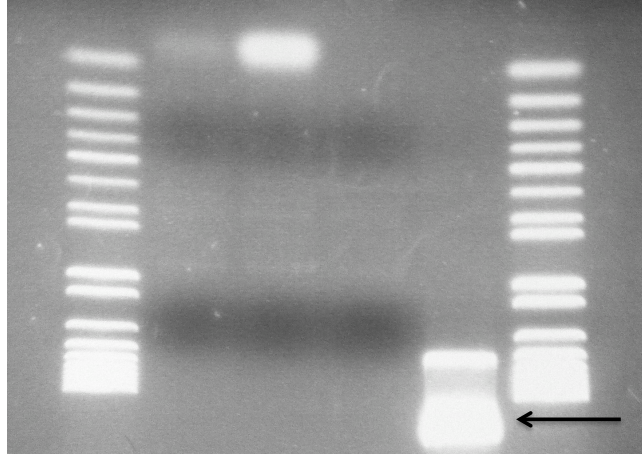


**Figure 3-1. Analysis by agarose gel electrophoresis of SpcN<sup>WT</sup> mutagenesis product.**

The lanes from left to right contain the 1Kb+ ladder, positive control, negative control, PCR product from 125 ng of template, PCR product from 31 ng of template. Significant primer dimer formation is observed.

### **3.1.2 Purification of SpcN<sup>WT</sup>**

Overexpression of SpcN<sup>WT</sup> is mostly insoluble, with only a fraction of the enzyme that is expressed in soluble form (figure 3-2). Nevertheless, we wanted to use SpcN<sup>WT</sup> to assess the feasibility of alternative methods to affinity purification. We sequentially purified SpcN<sup>WT</sup> using FPLC ion-exchange and size-exclusion chromatography methods. As anticipated, the purification yield of SpcN<sup>WT</sup> was quite low at approximately 0.41 mg of pure enzyme per liter of culture. Qualitative analysis by SDS-PAGE shows two bands (figure 3-3). One band at 35 kDa corresponds to SpcN<sup>WT</sup> and the other band is approximately 20 kDa. The second band consistently showed up throughout the purification. An additional step of size exclusion chromatography would be required, but was not possible given the low purification yield.

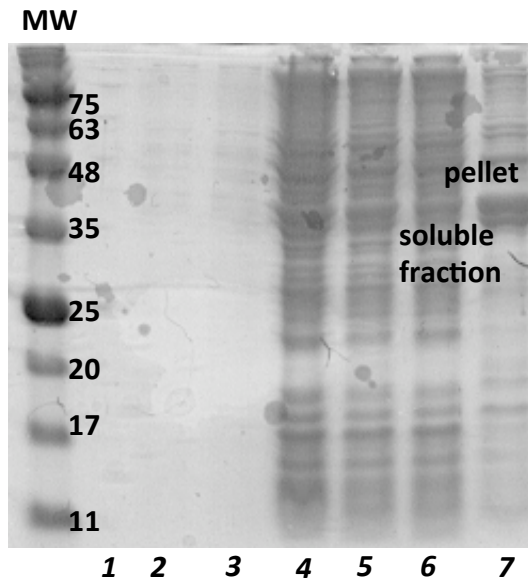


**Figure 3-2. SDS-PAGE analysis of SpcN<sup>WT</sup> overexpression in *E. coli*.**  
**1:** pre-induction culture; **2:** 2 hr 20 min induction, 37°C; **3:** 2 hr 40 min induction, 37°C;  
**4:** whole cell lysate 1; **5:** whole cell lysate 2; **6:** soluble fraction; **7:** pellet.

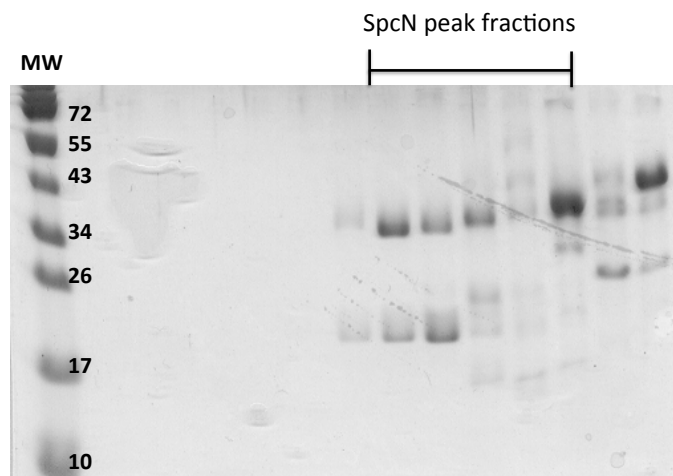


**Figure 3-3. SDS-PAGE analysis of SpcN<sup>WT</sup> following sequential Q-Sepharose and S-Sepharose ion-exchange chromatography.**

### **3.1.3 Overexpression and Solubilization of SpcN<sup>WT</sup>**

The insolubility of the SpcN<sup>WT</sup> when overexpressed in *E. coli* BL21(DE3) poses major hurdles for purification and crystallization of this enzyme. Solubility is often an issue when overexpressing recombinant protein in *E. coli*. SpcN<sup>WT</sup> has been isolated exclusively from *Streptomyces* species; it is therefore possible that *E. coli* cannot support overexpression of the enzyme (Lutzkanova *et al*, 1997). Common strategies for improving solubility target overexpression parameters. These include induction temperatures, growth media, concentration of inducing agent, induction time, host cell line, introduction of an epitope tag, changing the location of an epitope tag within the gene, *E. coli*-specific codon optimization of the gene, and stimulating up-regulation of protein folding machinery prior to protein expression.

In an effort to increase the yield of soluble enzyme, we modified several parameters during SpcN<sup>WT</sup> overexpression (Section 2.1.3). We tested the effects of lysis methods, host cell lines, induction temperatures, concentrations of inducing agent, growth media, induction times, and presence of solubilization agents. Qualitative analysis by SDS-PAGE of SpcN<sup>WT</sup> solubility generally showed no significant improvement over the original expression conditions (figure 3-4a). The presence of BugBuster<sup>®</sup> 10X in the lysis buffer was the only parameter for which solubility was significantly improved (figure 3-4b). BugBuster<sup>®</sup> 10X is a reagent prepared by Novagen that lyses cells by chemically disrupting their cell wall. In contrast to mechanical lysis methods, it is considered a much gentler approach for the release of overexpressed protein from the cell. SpcN<sup>WT</sup> is likely an unstable protein when expressed in *E. coli*, and protein denaturation occurs readily when cells are lysed mechanically. This could be a result of the increase in temperature that occurs during sonication for example. Therefore chemical lysis, which poses significantly less trauma to cell contents during lysis, would allow recombinant proteins to retain their stability and solubility.

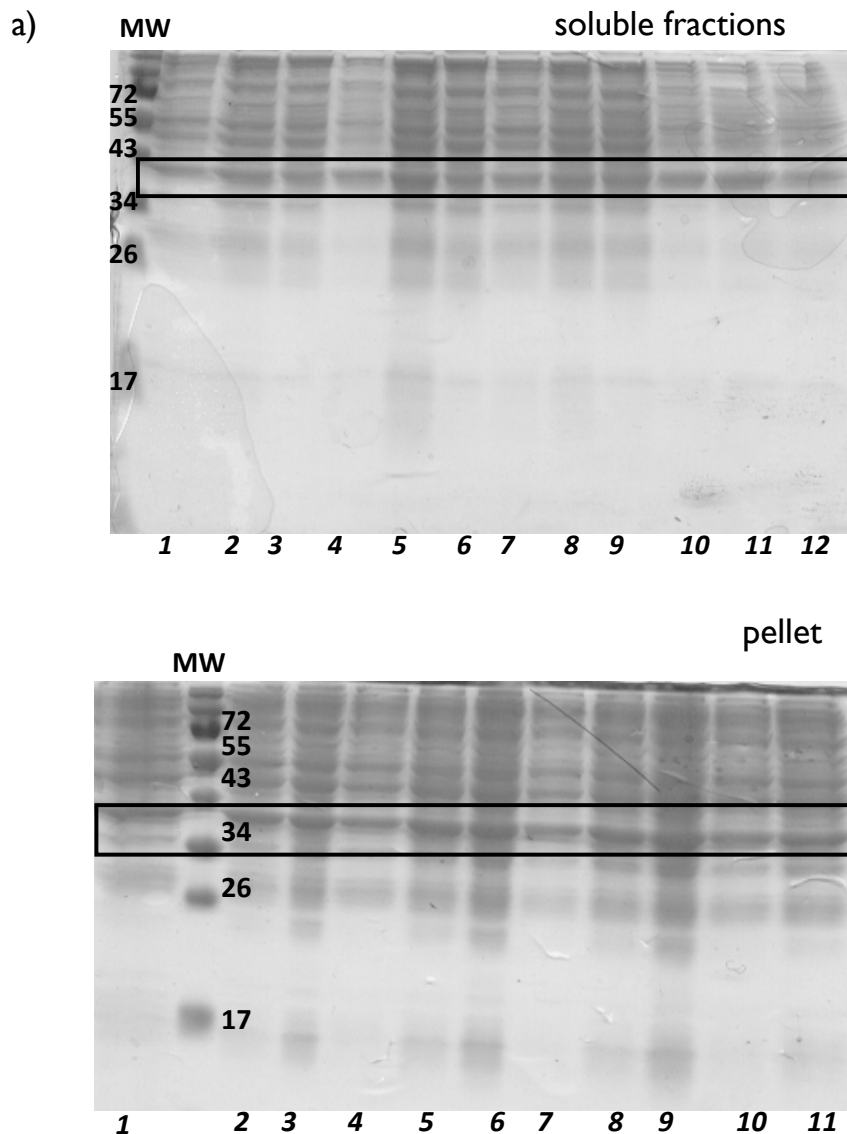


**Figure 3-4a. Sample SDS-PAGE analysis of SpcN<sup>WT</sup> solubility tests (lysis by sonication).**

IPTG concentration and induction times were **1:** 1 mM, 2 hrs; **2:** 1 mM, 5 hrs; **3:** 1 mM, 16 hrs; **4:** 0.5 mM, 2 hrs; **5:** 0.5 mM, 5 hrs; **6:** 0.5 mM, 16 hrs; **7:** 0.1 mM, 2 hrs; **8:** 0.1 mM, 5 hrs; **9:** 0.1 mM, 16 hrs; **10:** 0.01 mM, 2 hrs; **11:** 0.01 mM, 5 hrs; **12:** 0.01 mM, 16 hrs. Induction temperature was 37°C for this sample.

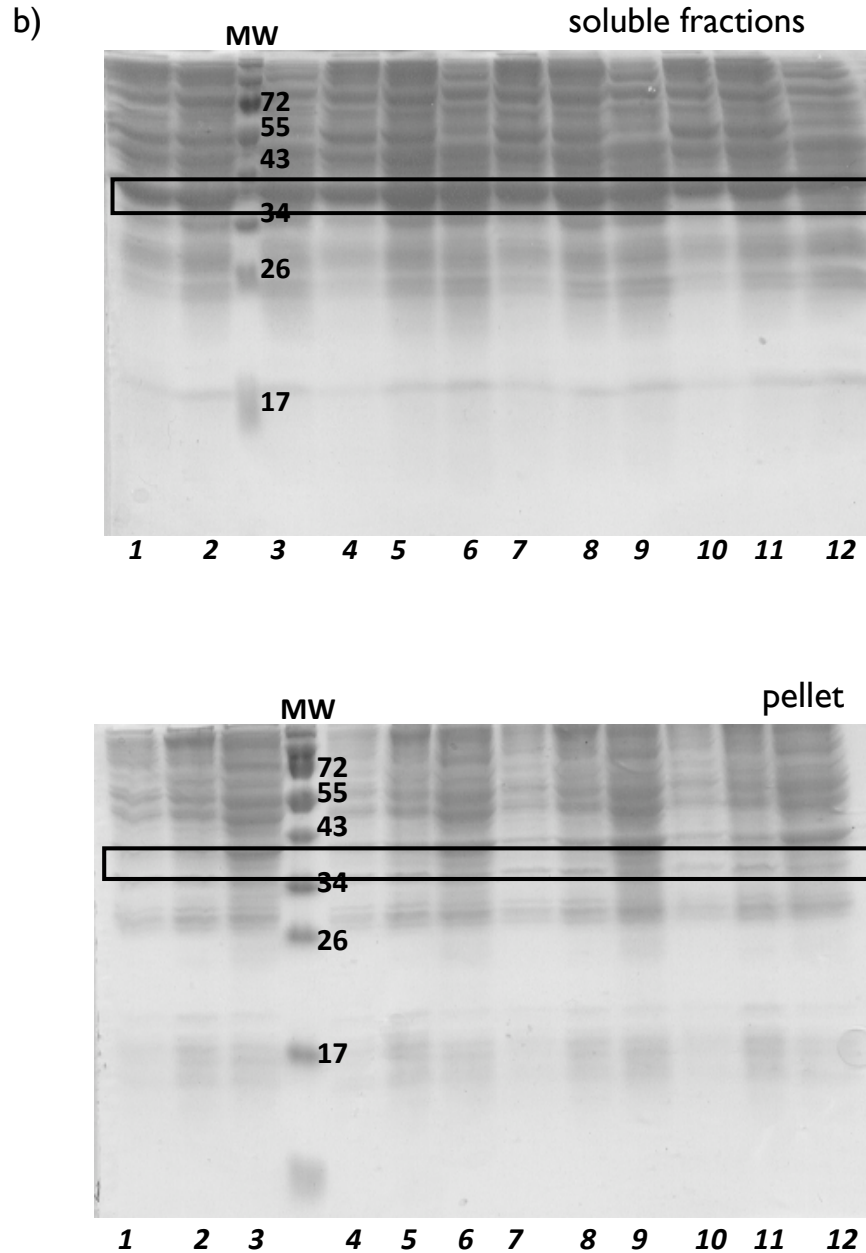


**Figure 3-4b. Sample SDS-PAGE analysis of SpcN<sup>WT</sup> solubility tests (lysis by BugBuster<sup>®</sup>).**

IPTG concentration and induction times were **1:** 1 mM, 2 hrs; **2:** 1 mM, 5 hrs; **3:** 1 mM, 16 hrs; **4:** 0.5 mM, 2 hrs; **5:** 0.5 mM, 5 hrs; **6:** 0.5 mM, 16 hrs; **7:** 0.1 mM, 2 hrs; **8:** 0.1 mM, 5 hrs; **9:** 0.1 mM, 16 hrs; **10:** 0.01 mM, 2 hrs; **11:** 0.01 mM, 5 hrs; **12:** 0.01 mM, 16 hrs. Induction temperature was 37°C for this sample.

### **3.1.4 Pyruvate Kinase/Lactate Dehydrogenase-Coupled Activity Assay**

Protein activity was monitored by a continuous pyruvate kinase/lactate dehydrogenase coupled assay (Gosselin *et al.*, 1994; McKay *et al.*, 1994). SpcN catalyzes the ATP-dependent phosphorylation of spectinomycin. The ADP generated by SpcN undergoes a phosphoenolpyruvate (PEP)-mediated phosphorylation by pyruvate kinase (PK), using to generate pyruvate. Lactate dehydrogenase converts pyruvate to lactate through oxidation of NADH. The decrease in NADH can be monitored spectrophotometrically by a decrease in absorbance at 340 nm. The assay was done on 0.41 mg/ml of purified SpcN<sup>WT</sup>, which is much lower than the average concentration of enzyme used for this assay (Gosselin *et al.*, 1994; McKay *et al.*, 1994). It was therefore not surprising that no activity was detected throughout the assay (figure 3-5).

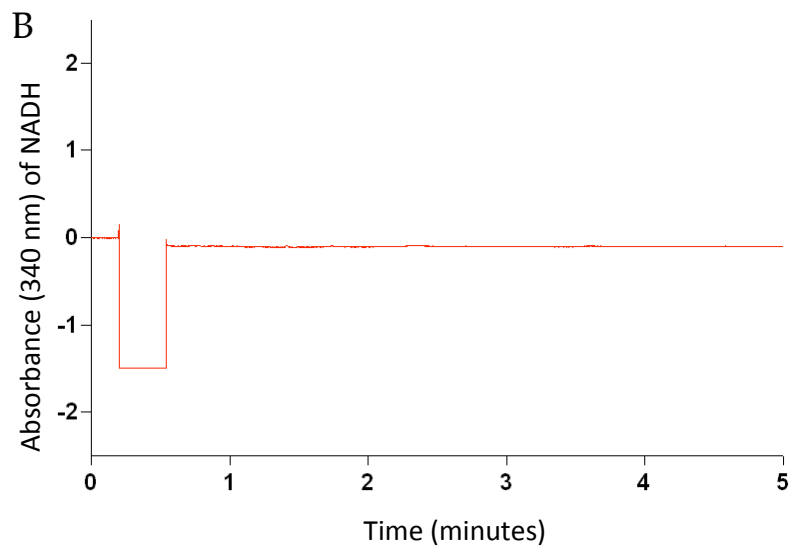
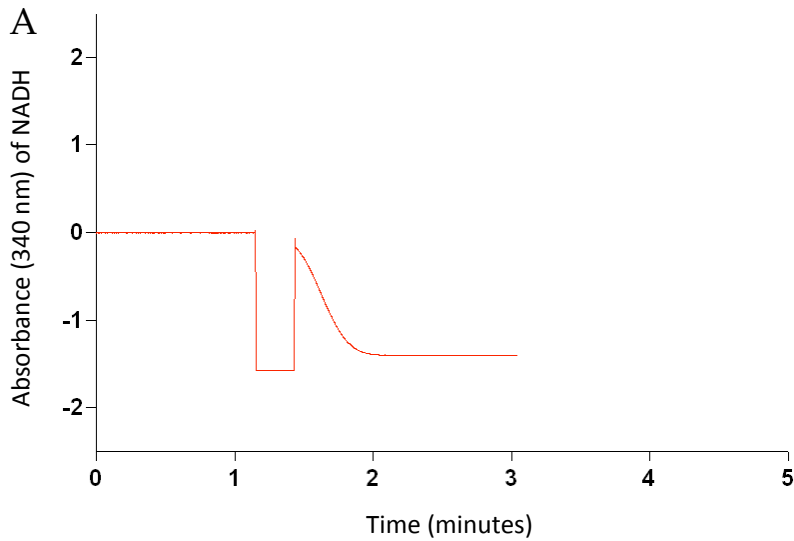


**Figure 3-5. Continuous PK/LDH-coupled activity assay monitoring the decrease in absorbance of NADH upon oxidation.**

A) positive control; ADP was added to start the reaction; B) Activity of 0.41 mg/ml SpcN<sup>WT</sup>. The sharp dip in absorbance observed upon addition of either ADP (positive control) or SpcN<sup>WT</sup> is due to light interference from opening the lid of the spectrophotometer.

## **3.2. Aminoglycoside Nucleotidyltransferase (2'')-Ia**

### **3.2.1 Refolding Purification of ANT(2'')-Ia<sup>XL</sup>**

In order to purify ANT(2'')-Ia<sup>XL</sup> from inclusion bodies, we adapted the refolding protocol established by Serpersu *et al* (Wright & Serpersu, 2004). To optimize overexpression for yield and time efficiency, preliminary induction tests investigated IPTG concentration, induction times and induction temperature (section 2.2.4.1).

We observed that protein concentration increased with decreasing IPTG concentrations. This is not uncommon, as overloading of the cell and transcriptional machinery can hinder protein expression (Malakar & Venkatesh, 2012). The amount of ANT(2'')-Ia<sup>XL</sup> overexpressed did not significantly change after 3 hrs of induction, and incubating overnight produced more impurities without improving ANT(2'')-Ia<sup>XL</sup> yield. This is to be expected since activity of the inducible promoter likely plateaus and expression of native proteins in *E. coli* cells continues for an extended period of time. Induction at 15°C consistently produced low yields of ANT(2'')-Ia<sup>XL</sup>, but induction at 30°C and 37°C produced comparable amount of protein after 2 hrs of induction.

Based on these observations, we adjusted the overexpression parameters proposed by Serpersu *et al* from 6 hours of induction to 3 hours, while keeping the induction temperature and final IPTG concentrations at 37°C and 0.05 mM IPTG (Wright & Serpersu, 2004). This allowed for better time efficacy in the overexpression and purification protocol (data not shown).

Though a large amount of protein is expressed upon induction, the majority forms inclusion bodies. Serpersu *et al* optimized the refolding protocol for two forms of ANT(2'')-Ia<sup>XL</sup> that resulted in a high yield of 74-91 mg of ANT(2'')-Ia<sup>XL</sup> per liter of culture with a percent recovery (after refolding) of over 95% (Serpersu, 2004). The two forms discussed consist of a 249 amino acid protein with a reported molecular weight of 35 kDa, and a 226 amino acid protein with a reported molecular weight of 29 kDa. It has been suggested that these two forms result from the presence of two different start codons

within the same open reading frame. The shorter form was found to show higher expression levels and percent recovery after refolding (Serpersu 2004).

We obtained an overall yield of 72.5 mg of pure ANT(2'')-Ia<sup>XL</sup> from 1L of culture (figure 3-6). This is consistent with the yield reported in literature (Serpersu, 2004). Qualitative analysis of purified ANT(2'')-Ia<sup>XL</sup> by SDS-PAGE shows very pure protein comparable to that reported by Serpersu *et al.* SDS-PAGE analysis also confirmed a molecular weight of 26 kDa, which is consistent with the molecular weight predictions based on the sequence.

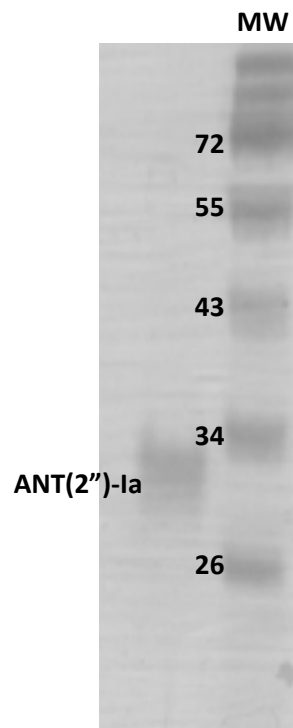


**Figure 3-6. SDS-PAGE analysis of final product following refolding protocol.**

ANT(2'')-Ia<sup>XL</sup> was concentrated to 6 mg/ml.

### **3.2.2 Nucleotidyltransferase Activity Assay on ANT(2'')-Ia<sup>XL</sup>**

Protein activity was monitored by a discontinuous nucleotidyltransferase activity assay (Serpensu *et al.*, 2008). Inorganic pyrophosphate is the product of the ATP dependent adenylation of 2-hydroxyaminoglycosides. The increase in levels of inorganic phosphate upon hydrolysis of inorganic pyrophosphate by pyrophosphatase is measured spectrophotometrically at 820 nm.

Two negative controls were used; the first substituted the aminoglycoside ligand for water, and the second consisted of pyrophosphate alone (in the absence of pyrophosphatase) to verify for phosphate contamination. One positive control was used, consisting of both pyrophosphate and pyrophosphatase together. Tobramycin was used for the aminoglycoside ligand. The activity of purified ANT(2'')-Ia<sup>XL</sup> stored for over 24hrs at both -80°C and 4°C was tested. Activity was also tested for fresh samples within 24hrs of refolding.

Marginal activity was detected for samples stored for less than 24 hrs, but it remained significantly weaker than the positive control (figure 3-7). All samples stored at both -80°C and 4°C showed no activity when tested again less than a week later, confirming that activity for refolded ANT(2'')-Ia<sup>XL</sup> is not stable, which is consistent with literature (Ekman *et al.*, 2001).

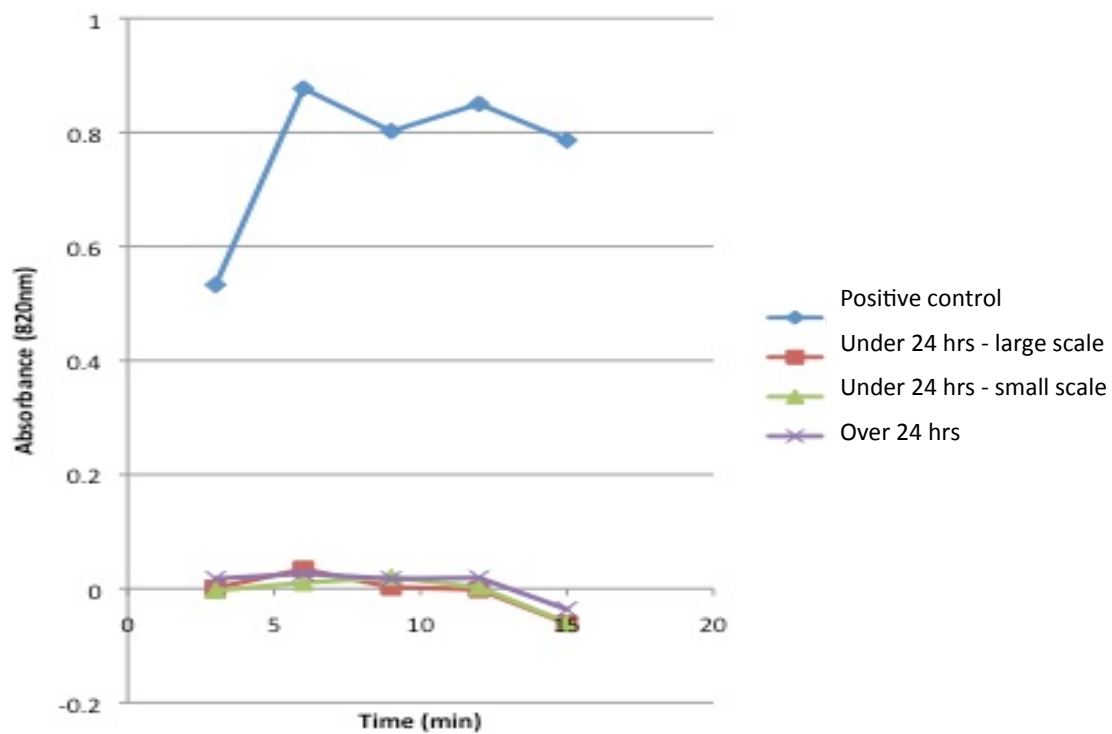


**Figure 3-7. Activity assays for ANT(2'')-Ia<sup>XL</sup> refolded from inclusion bodies.**

Large-scale and small-scale refolding, stored at 4°C for under 24 hrs; small-scale refolding, stored at 80°C for over 24 hrs.

In order to perform structural studies on ANT(2'')-Ia<sup>XL</sup>, we needed pure and stable protein; which we determined could not effectively be obtain by refolding from inclusion bodies. We therefore attempted to optimize parameters for ANT(2'')-Ia<sup>XL</sup> overexpression so that we could explore alternative purification methods. No improvement in solubility however was observed for all conditions tested (figure 3-8). We therefore proceeded to investigate construct of ANT(2'')-Ia<sup>XL</sup>.

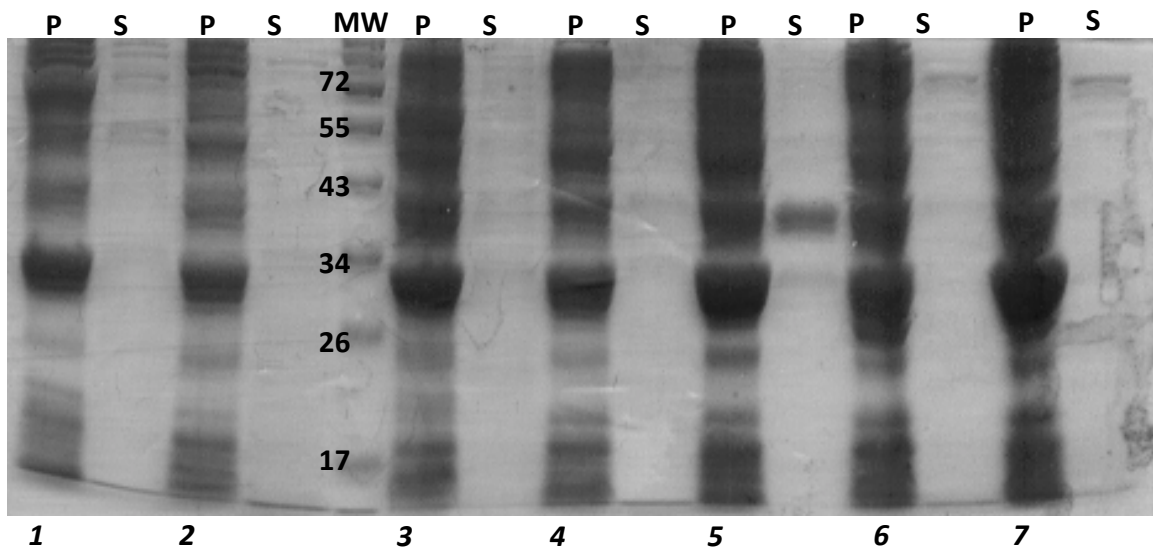


**Figure 3-8. Sample SDS-PAGE analysis of solubility test on ANT(2'')-Ia<sup>XL</sup>.**

This figure shows expression in various cell lines screened after 1 hour of induction. **1:** Arctic Express, 10°C; **2:** BB101, 15°C; **3:** BB101, 37°C; **4:** BL21(AI), 15°C **5:** BL21(AI), 37°C; **6:** Rosetta(DE3), 15°C; **7:** Rosetta(DE3), 37°C.

### **3.2.3 Sequence Analysis, Cloning and Mutagenesis of ANT(2'')-Ia<sup>XL</sup>**

Sequencing of *ANT(2'')-Ia<sup>XL</sup>* confirmed that the construct we obtained is consistent with the 226 amino acid form of *ANT(2'')-Ia<sup>XL</sup>* found in literature (Cameron *et al.*, 1986). A Position-Specific Iterative (PSI)-BLAST done on *ANT(2'')-Ia<sup>XL</sup>* highlighted a significant difference between the *ANT(2'')-Ia* sequence and related sequences in the database. We observed that the majority of *ANT(2'')-Ia* related sequences lacked the first 49 amino acids at the N-terminus that were present in our construct. Also, the *ANT(2'')-Ia* sequence possesses an alternative start-codon at that position. This suggested that the first 49 amino acids were potentially obsolete and might be responsible for the instability of the *ANT(2'')-Ia<sup>XL</sup>* construct. To investigate this possibility, we cloned a new construct, *ANT(2'')-Ia<sup>SC</sup>*, omitting the sequence coding for the first 49 amino acids of *ANT(2'')-Ia<sup>XL</sup>* (section 2.2.2). Analysis by agarose gel electrophoresis of double-digested *ANT(2'')-Ia<sup>SC</sup>* showed an insert between 500 and 600 bp, confirming a change in gene length from 678 bp (*ANT(2'')-Ia<sup>XL</sup>*) to 531 bp (*ANT(2'')-Ia<sup>SC</sup>*).

The *ANT(2'')-Ia<sup>SC</sup>* construct includes an additional leucine and glutamic acid from the pET22(b)+ vector that were incorporated between the end of the *ANT(2'')-Ia<sup>SC</sup>* gene and the 6XHis tag. Excluding the hexahistidine tag, it contains 177 amino acids, has a molecular weight of 20.9 kDa and an extinction coefficient of 49,180 M<sup>-1</sup>cm<sup>-1</sup>.

### **3.2.4 Overexpression and purification of ANT(2'')-Ia<sup>SC</sup>**

*ANT(2'')-Ia<sup>SC</sup>* was successfully overexpressed in BL21(DE3) cells and purified by nickel affinity chromatography (section 2.2.4.2). The UV trace for this purification showed that *ANT(2'')-Ia<sup>SC</sup>* elutes around 10-30% of high imidazole buffer ("B") into two major peaks and one minor peak with a negligible UV absorbance (figure 3-9). Qualitative analysis by SDS-PAGE following affinity chromatography shows that *ANT(2'')-Ia<sup>SC</sup>* is relatively pure but still with another band (figure 3-10).

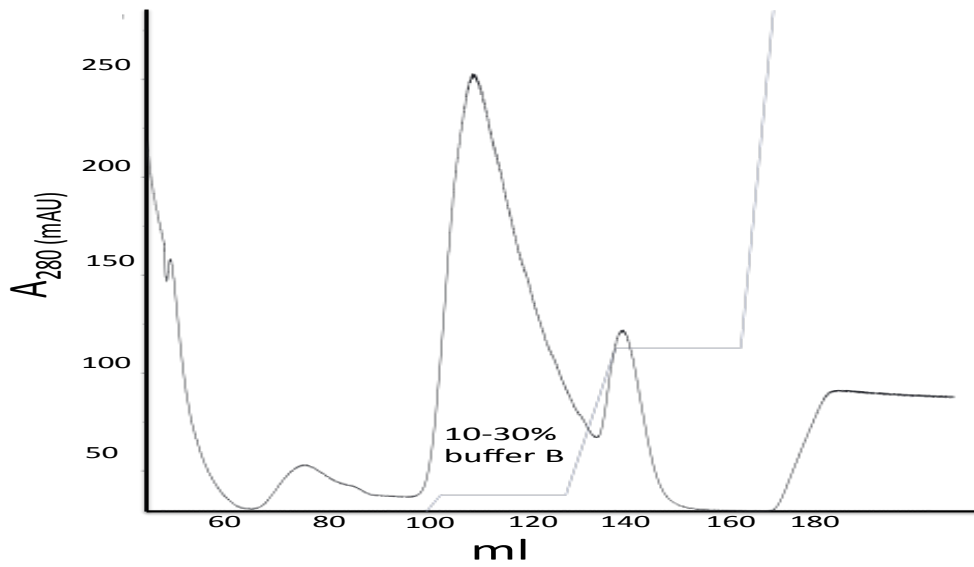


**Figure 3-9. Elution profile for the first purification step by nickel affinity chromatography on a Qiagen 5 ml Ni-NTA Superflow Cartridge.**

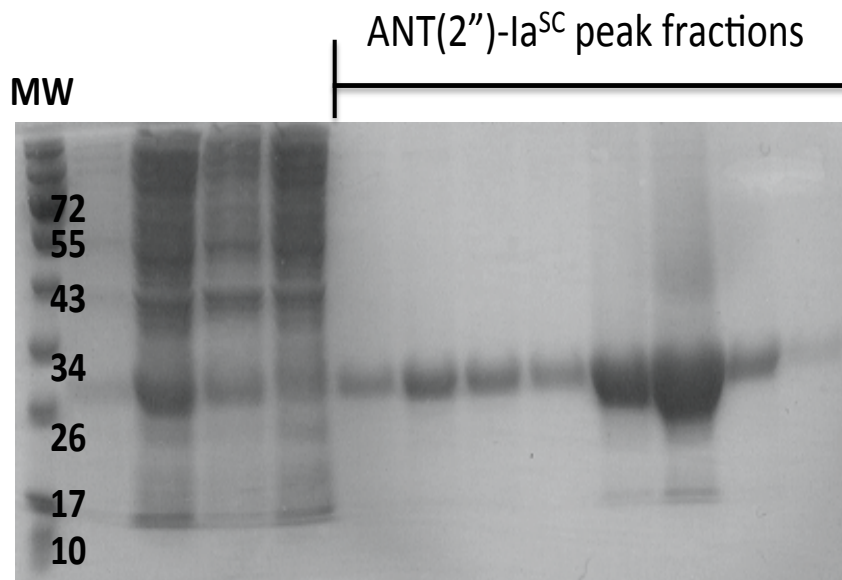


**Figure 3-10. Qualitative analysis by SDS-PAGE of ANT(2'')-Ia<sup>SC</sup> fractions and relative purity after nickel affinity chromatography.**

To increase protein purity to a level sufficient for structural studies, ANT(2'')-Ia<sup>SC</sup> was further purified by size exclusion chromatography on a Qiagen HiLoad 26/50 Superdex 75 column. The elution profile showed a single peak with high UV absorbance which eluted over 40 mL after 133.5 mL of void volume (figure 3-11).

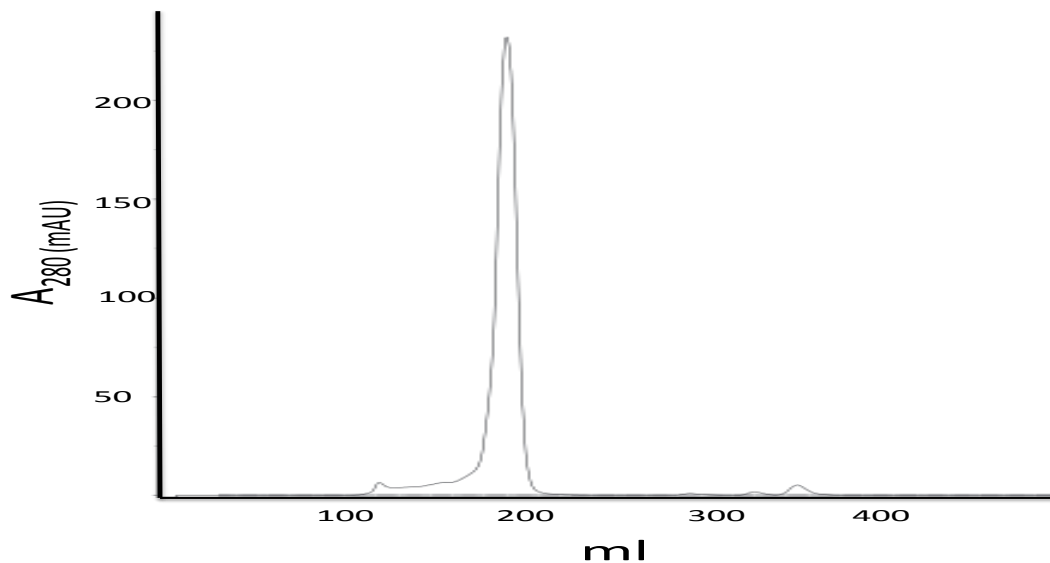


**Figure 3-11. Elution profile for the second purification step by size exclusion chromatography on a Qiagen HiLoad 26/50 Superdex 75 column.**

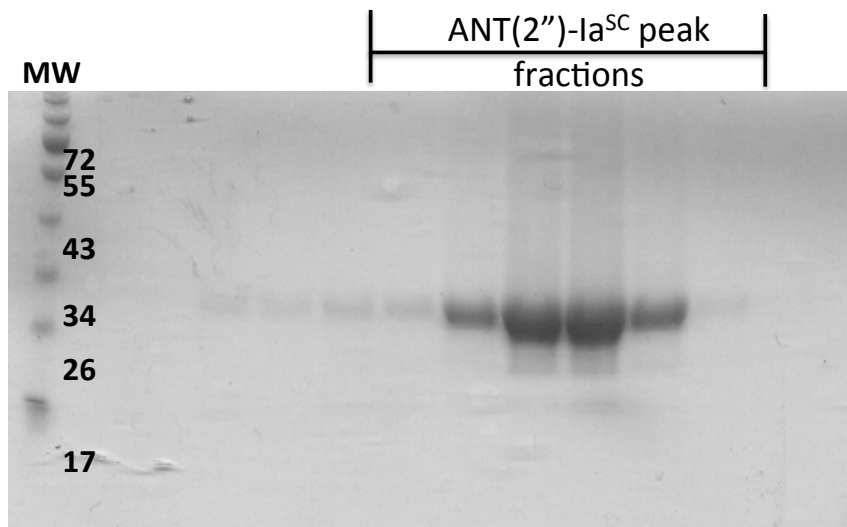


**Figure 3-12. Qualitative analysis by SDS-PAGE of ANT(2'')-Ia<sup>SC</sup> fractions and relative purity after both nickel affinity chromatography and size exclusion chromatography.**

The sequential purification of ANT(2'')-Ia<sup>SC</sup> by affinity chromatography and size exclusion chromatography results in 17 mg of pure enzyme per liter of cell culture pure protein. The degree of purity was qualitatively assessed by SDS-PAGE (figure 3-12).

### **3.2.5 Nucleotidyltransferase Activity Assay on ANT(2'')-Ia<sup>SC</sup>**

The same discontinuous nucleotidyltransferase activity assay and controls used for ANT(2'')-Ia<sup>XL</sup> was used for ANT(2'')-Ia<sup>SC</sup> (section 3.2.2). We used this assay to qualitatively assess protein activity by spectrophotometrically measuring at 820 nm the amount of inorganic phosphate produced as compared to the control. To investigate the effects of protein concentration and buffer pH on activity, three samples of ANT(2'')-Ia<sup>SC</sup> were tested: 1) pH 6.8 with a concentration of 2.3 mg/mL, 2) pH 8.0 with a concentration of 11.3 mg/mL, 3) pH 8.0 with a concentration of 1.0 mg/mL. All samples showed significant activity above the base line. The samples were tested again after 6 days, and protein activity remained stable (Figure 3-13).

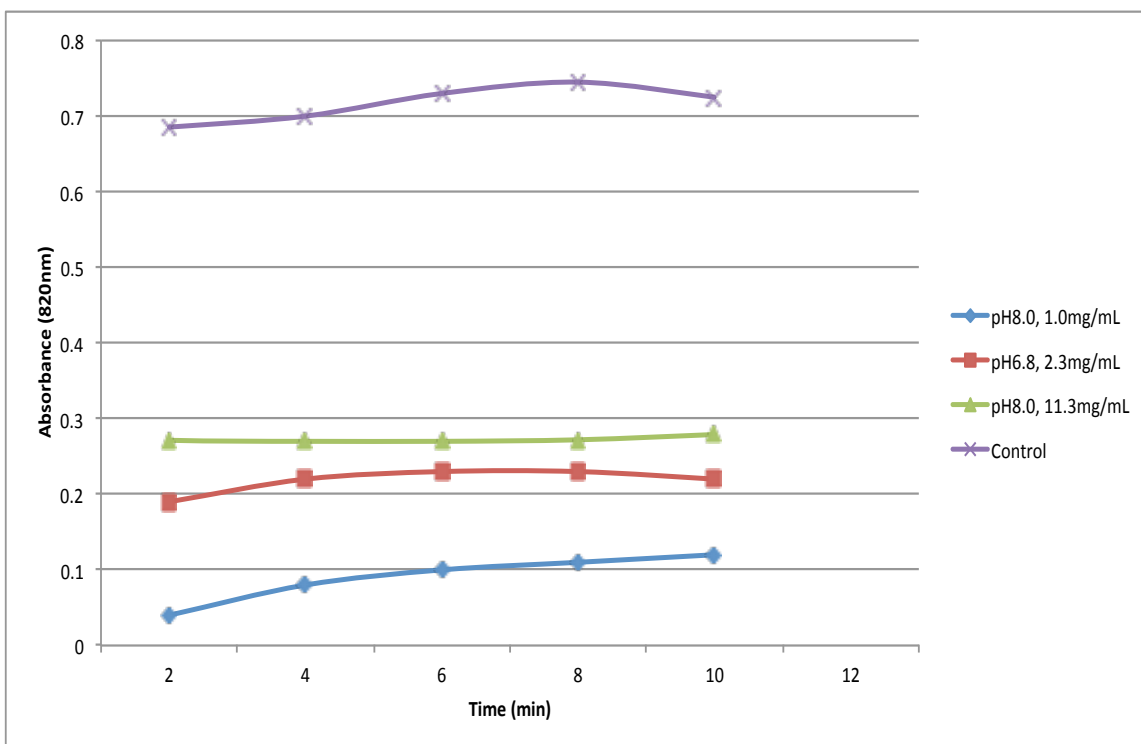


**Figure 3-13. Activity assays for ANT(2'')-Ia<sup>SC</sup> following FPLC Ni-NTA and size-exclusion chromatography.**

### **3.2.6 Nuclear Magnetic Resonance (NMR) Experiments of ANT(2'')-Ia<sup>SC</sup>**

In addition to providing important structural information, studies using NMR offer insight into macromolecular dynamics and folding properties of the protein being studied. Though molecular weight can be a limiting factor in NMR experiments, the size of the ANT(2'')-Ia<sup>SC</sup> protein construct falls within the acceptable range, allowing us to explore NMR as a possibility for structural studies (Yu, 1999).

Given the high sensitivity of NMR probes, the protein that was purified specifically for NMR studies was eluted in a buffer adjusted to improve signal detection (50 mM Tris-HCl, 50 mM NaCl, pH 7.0). The salt concentrations were decreased to ensure less conductivity and therefore higher sensitivity of the probe (Kelly *et al.*, 2002; Kovacs *et al.*, 2005). The pH was also lowered from 8.0 to 7.0 to slow the base-catalyzed exchange rates of the backbone amide protons.

Proper protein folding was assessed by  $^{15}\text{N}$ -HSQC NMR on 0.7 mM  $^{15}\text{N}$ -ANT(2'')-Ia in 50 mM Tris-HCl, 50 mM NaCl, pH 7.0 at 30°C. The HSQC spectrum showed sharp peaks with broad chemical shift dispersion, confirming that the protein was homogeneous and properly folded (figure 3-14).

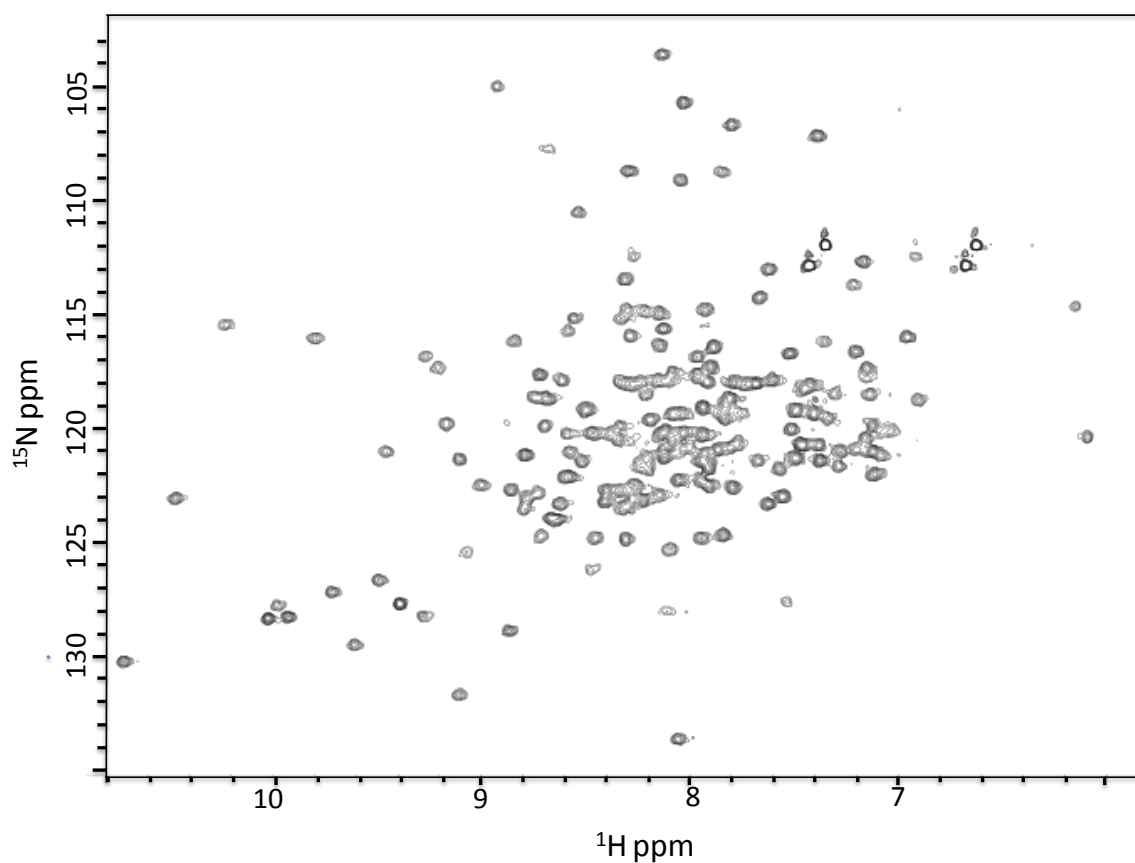


**Figure 3-14  $^{15}\text{N}/^1\text{H}$  HSQC spectrum of ANT(2'')-Ia<sup>SC</sup> showing sharp peaks and broad chemical shift dispersion.**

The Sparky program identified 166 of the 190 non-proline resonance peaks. Exchange rates for the amide backbone protons are not uniform throughout the entire protein, therefore some peak broadening was observed which resulted in peak overlaps. This mostly accounted for the fact that the Sparky program did not identify the remaining 24 non-proline peaks.

### *Sequential backbone assignment of ANT(2'')-Ia<sup>SC</sup>*

We collected data for HNCACB and CBCAcoNH triple resonance experiments on 0.7 mM <sup>15</sup>N,<sup>13</sup>C-ANT(2'')-Ia<sup>SC</sup> in 50 mM Tris-HCl, pH 7.0, 50 mM NaCl at 30°C for the sequential backbone assignment of our enzyme. In contrast to the HSQC spectrum, which had sharp and well-dispersed resonance peaks (figure 3-14), the peaks in the CBCAcoNH and HNCACB spectra were generally weak (or absent for many amino acids), exhibited peak broadening and chemical shift degeneracy. We were able to assign 144 of the 166 non-proline amide peaks on the HSQC spectrum (figure 3-15).

In order to fully assign the amide backbone, higher resolution spectra are required for the HNCACB and CBCAcoNH triple resonance experiments. To increase spectral resolution, buffer content, buffer pH, temperature should first be optimized. We performed all experiments in Tris-HCl buffer at a pH of 7.0 exclusively. Tris-HCl buffers have relatively high conductivity when compared to other NMR buffers such as phosphate, acetate, or Bis-Tris buffers for example (Kelly *et al.*, 2002). If ANT(2'')-Ia<sup>SC</sup> can remain stable in these alternative buffers, they should be considered for future NMR experiments. Also, more acidic pHs should be considered, if protein stability permits, to further decrease the amide backbone proton exchange rates and improve signal resolution. Finally, signal resolution can be greatly improved by increasing the temperature for NMR experiments. We collected preliminary HSQC data for 0.2 mM ANT(2'')-Ia<sup>SC</sup> at varying temperatures and observed no significant changes in signal resolution (data not shown). Additional temperature optimization experiments need to be done on 0.7 mM ANT(2'')-Ia<sup>SC</sup>.

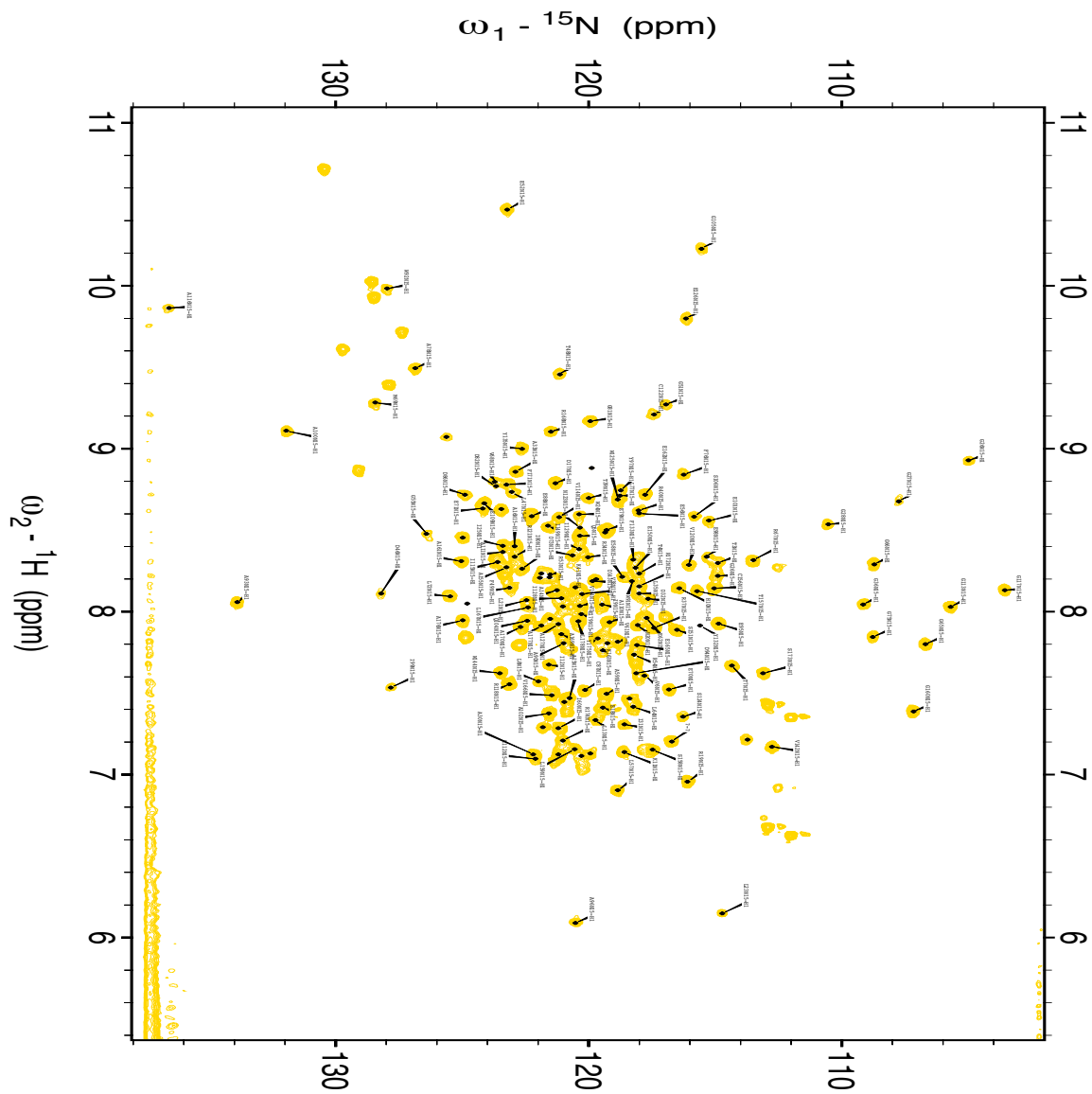
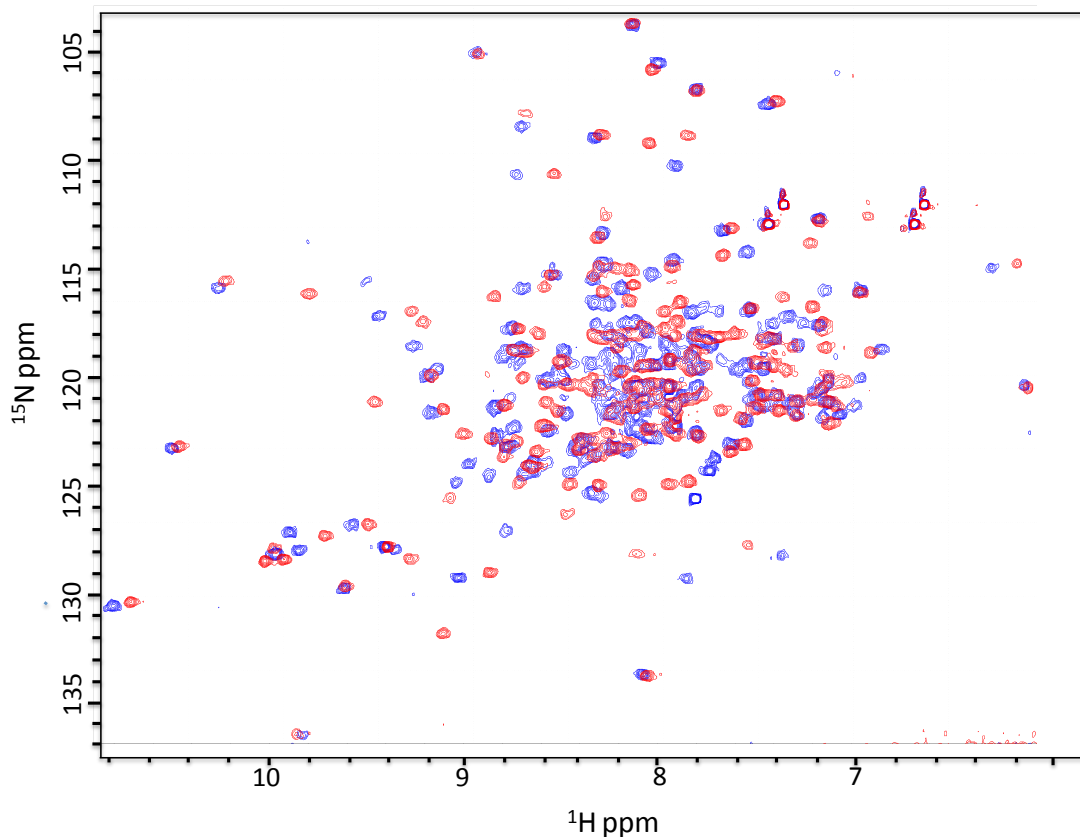


**Figure 3-15. Assigned HSQC spectrum for ANT(2'')-Ia<sup>SC</sup>.**

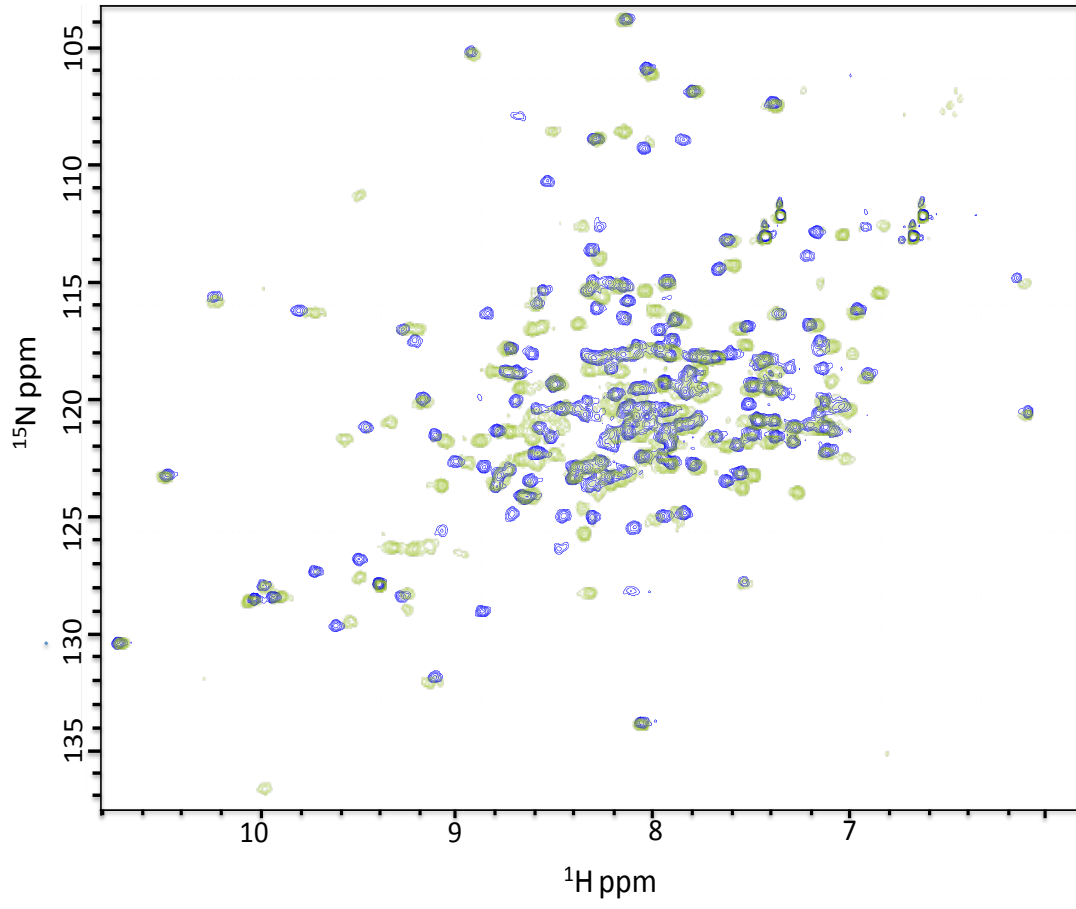
### *Analysis of chemical shift perturbations upon ligand binding*

To study the binding dynamics and specificities of ANT(2'')-Ia<sup>SC</sup> and its substrates, interactions with both tobramycin and ATP were studied separately by HSQC titration experiments. Comparison of HSQC spectra of the two ligand-bound ANT(2'')-Ia<sup>SC</sup> with free ANT(2'')-Ia<sup>SC</sup> shows ligand-specific, global chemical shift perturbations (figure 3-16). Titration experiments with both ATP and tobramycin respectively were saturated at the molar ratio of 1:1 as we did not detect any further chemical shift perturbation at the next titration step, which was a molar ratio of 1:2. This indicates high-affinity interactions for both ligands with the stoichiometry of 1:1. The chemical shift perturbations may arise from the direct interaction of the ligand with specific amino acids or, indirectly from the conformational changes of the protein upon ligand binding.

a)



b)



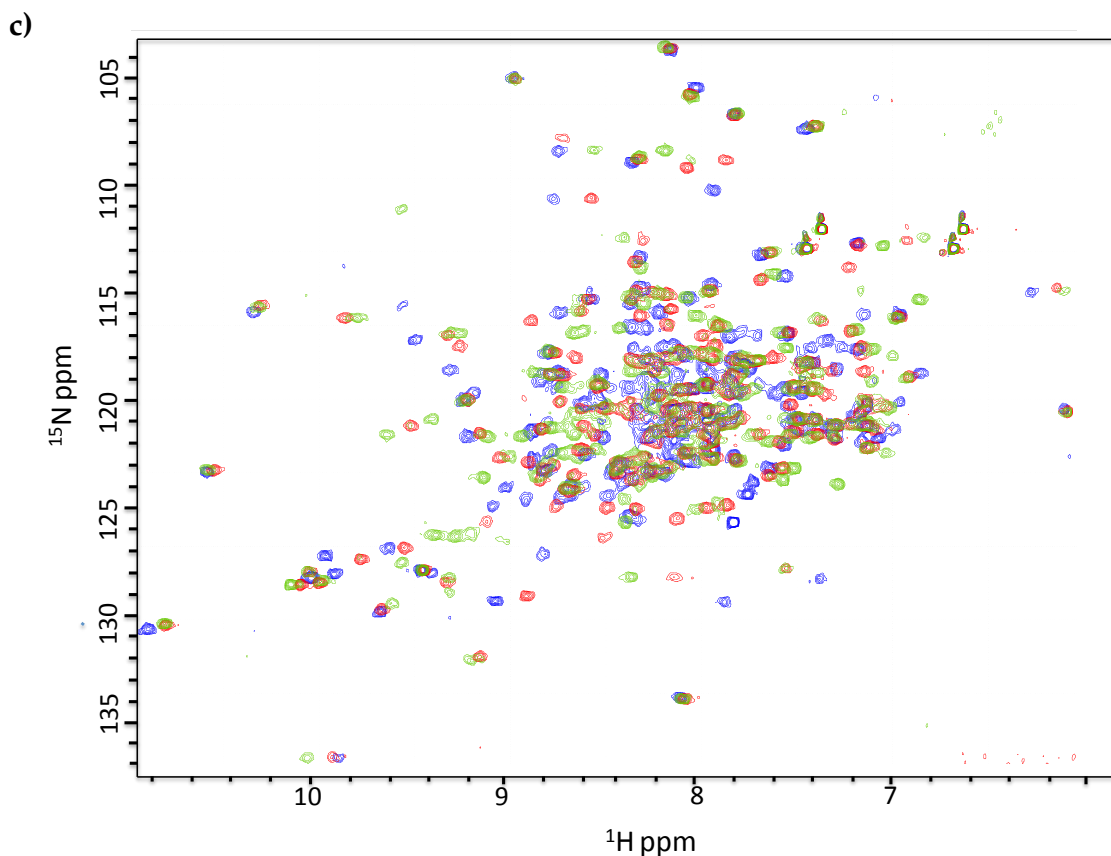


**Figure 3-16. Global chemical shift perturbations in  $^{15}\text{N}$ -HSQC spectra of substrate-bound ANT(2'')-Ia<sup>SC</sup> shown by overlapping with the spectrum of apo-ANT(2'')-Ia<sup>SC</sup>.**

**a)** 0.5 mM apo-ANT(2'')-Ia<sup>SC</sup> (blue) and tobramycin-bound ANT(2'')-Ia<sup>SC</sup> (red) at a 1:1 concentration ratio; **b)** 0.5 mM apo-ANT(2'')-Ia<sup>SC</sup> (blue) and ATP-bound ANT(2'')-Ia<sup>SC</sup> (green) a 1:1 ratio; **c)** apo-ANT(2'')-Ia<sup>SC</sup>, tobramycin-bound ANT(2'')-Ia<sup>SC</sup> (red), and ATP-bound ANT(2'')-Ia<sup>SC</sup> (green).

In order to gain insight into the interactions of both ATP and tobramycin separately with ANT(2'')-Ia<sup>SC</sup>, the weighted average of the chemical shift perturbations for each was plotted against the sequence of ANT(2'')-Ia<sup>SC</sup> (figure 3-17, 3-18). These analyses show that the chemical shifts perturbations for each substrate bound spectrum (ANT(2'')-Ia<sup>SC</sup>-tobramycin and ANT(2'')-Ia<sup>SC</sup>-ATP) completely differ from each other. This suggests that

ATP and tobramycin bind at non-overlapping sites, and that ANT(2'')-Ia<sup>SC</sup> has two different binding pockets for the two substrates. This correlates with the Theorell-Chance binding mechanism proposed for ANT(2'')-Ia in literature (Gate & Northrop, 1988). Furthermore, the significant chemical shift perturbations for each ligand-bound spectrum suggest global conformational changes of the protein upon binding. They are also consistent with previous kinetic studies done on ANT(2'')-Ia, where increases in pKa and major changes in protonation states within the enzyme were reported (figure 3-19).

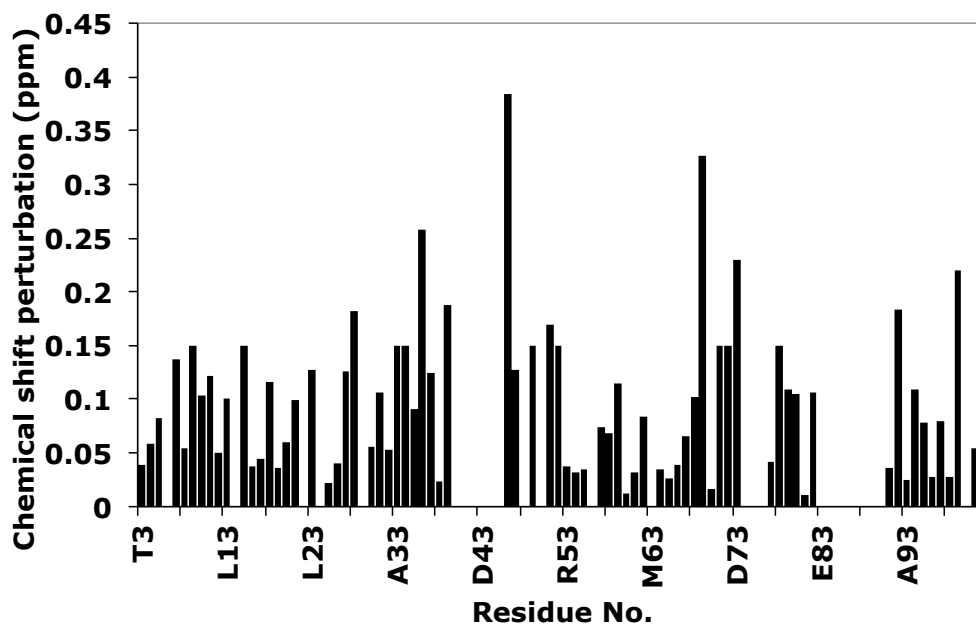


**Figure 3-17. Weighted average of the chemical shift perturbations for ANT(2'')-Ia<sup>SC</sup> titrated with tobramycin.**

The following amino acids disappeared from the spectra upon addition of substrate: V6, K11, A33, R40, T48, G55, E56, L72, G75, A100, V114, E126, Y135, A176.

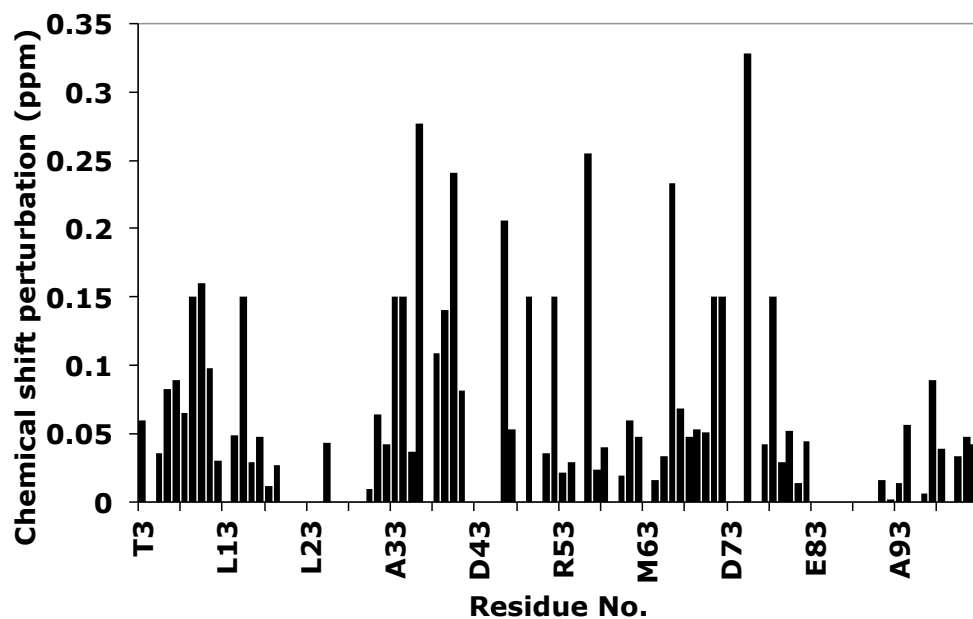


**Figure 3-18. Weighted average of the chemical shift perturbations for ANT(2'')-Ia<sup>SC</sup> titrated with ATP.**

The following amino acids disappeared from the spectra upon addition of substrate: L23, G27, G28, R34, T48, G55, D73, F76, D86, I129.

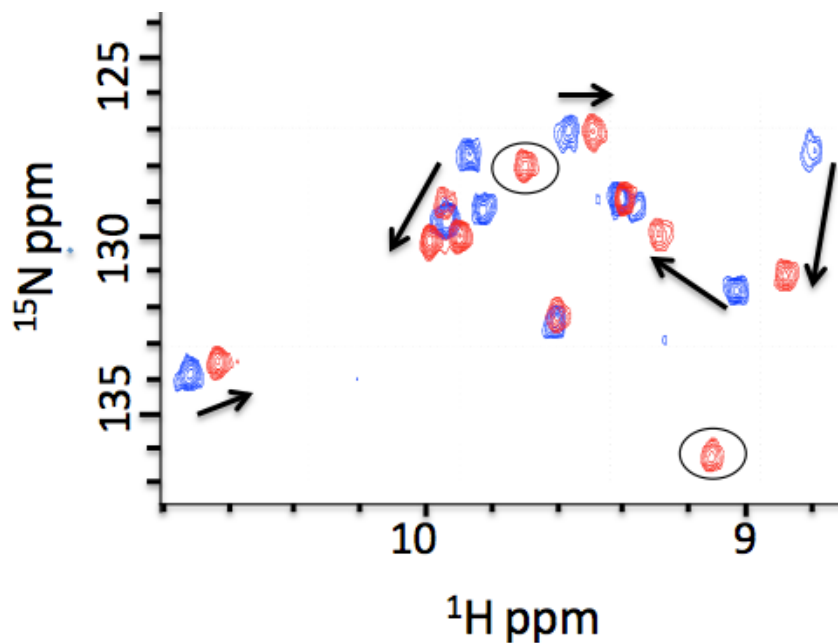


**Figure 3-19. Example of major chemical shift perturbations observed upon substrate binding.**

Section of the HSQC spectra of apo-ANT(2'')-Ia<sup>SC</sup> (blue) overlaid with ATP-bound ANT(2'')-Ia<sup>SC</sup> (red). Changes in resonance peak chemical shifts are noted by arrows and appearance of new peaks are highlighted by circles.

The two ligand bound spectra that were used for the analysis of chemical shift perturbations were assigned by manually transposing each peak assignments from the apo-ANT(2'')-Ia<sup>SC</sup> onto each ligand bound HSQC spectrum. High resolution triple resonance data need to be collected for both ATP-bound and tobramycin-bound ANT(2'')-Ia<sup>SC</sup> to accurately assign HSQC spectrum for each and assess which amino acids are involved in substrate binding.

## **4. CONCLUSION**

## 4.1 Conclusion and future directions for SpcN

Since overexpression of SpcN<sup>TAG</sup> originally resulted in soluble protein and SpcN<sup>WT</sup> is highly insoluble when overexpressed, it is likely that the affinity tag on SpcN<sup>TAG</sup> contributes to its stability and solubility. This is not uncommon for epitope tags, though the reasons for which they improve solubility and stability are still relatively unknown. The small size of this affinity tag generally makes it an appealing choice (Walls & Loughran, 2011). However, in the case of SpcN<sup>TAG</sup> the presence of the tag appears to hinder crystal formation, and thrombin cleavage of the tag at the N-terminus has not been possible.

Issues with cleavage may be related to accessibility of the N-terminus, the type of cleavage enzyme being used, or steric hindrance caused by the affinity tag (Waugh, 2011).

To address the potential accessibility issues, mutagenesis was attempted in order to change the location of the hexahistidine tag to the C-terminus, though further optimization of mutagenesis parameters is required in order to achieve this. Alternatively, increasing the length of the linker may also improve on accessibility to the region for cleavage enzymes. It is important to note however, that if the tag is kept throughout crystallization, the linker should be short and rigid, rather than long and flexible, to ensure high quality crystals (Walls & Loughran, 2011).

With regards to optimizing the cleavage enzyme, future studies should explore the use of TEV proteases for cleavage of the affinity tag. This is especially relevant given that TEV proteases are known to be ideal for cleavage at the N-terminus (Waugh, 2011).

Finally, the hexahistidine tag itself, though small, could be responsible for the steric hindrance preventing proper cleavage (Waugh, 2011). Given that SpcN<sup>TAG</sup> has no solubility issues, the hexahistidine tag appears to be sufficient to enhance solubility and stability over SpcN<sup>WT</sup>. Though it is appealing to explore alternative affinity tags specific for solubility enhancement, any larger tag may actually create other issues with steric hindrance when attempting to cleave the tag prior to crystallization.

## 4.2 Conclusion and future directions for ANT(2'')-Ia<sup>SC</sup>

Overexpression of ANT(2'')-Ia<sup>WT</sup> has consistently resulted in the formation of inclusion bodies. For this reason, little work has been done on this clinically important resistance enzyme. The *ANT(2'')-Ia<sup>WT</sup>* gene construct encoded both a 226 amino acid version and a 249 amino acid version of the enzyme differing in the site of the start codon (Wright & Serpersu, 2004, 2005, 2006, 2011). Our studies on the 226 amino acid form of ANT(2'')-Ia<sup>WT</sup> show that the refolding protocol optimized by Serpersu *et al.* does not produce stable enough protein for structural studies. We also found that the first 49 amino acids encoded at the N-terminus appear to be extraneous to properly folded and functional ANT(2'')-Ia. The resulting 177 amino acid protein that we identified overexpressed as soluble, stable and active enzyme, and we believe it is physiologically most relevant. The *ANT(2'')-Ia* gene is encoded on plasmids and transposons and is therefore widely distributed among various bacterial strains. As a result, it is found with variety of genetic elements incorporated within the different gene constructs available. When considering the multiple potential start codons in the *ANT(2'')-Ia* gene, it becomes clear that previous groups have simply been working with the wrong construct.

Given the smaller size of the *ANT(2'')-Ia<sup>SC</sup>* construct (20.9 kDa) that we identified, it became possible to pursue structural studies by NMR. Generally smaller proteins yield better spectra resolution because they have lower rotational correlation times ( $\tau_c$ ). As molecular weight increases, so does the rotational correlation time, which can cause peak broadening and decrease the signal to noise ratio. Also, as the number of atoms in a protein increases, the number of resonance peaks recorded also increase, causing peak overlap and chemical shift degeneracy. Structural studies by NMR offer a good alternative to x-ray crystallography in situations where crystallography is not possible. NMR can also compliment crystallography by examining protein stability and studying binding interactions. It allows us to study protein dynamics in solution or in a solvent environment similar to physiological conditions.

Upon studying ANT(2'')-Ia<sup>SC</sup> using NMR, well dispersed peaks were observed and

144 of the 176 non-proline amide backbone resonance peaks were assigned.

Titration studies done with tobramycin and ATP separately reveal major chemical shift perturbations that occur upon binding of each substrate at high affinity. These results suggest that different residues contribute to the binding site of each substrate. Such is the case with ANT(4')-Ia, which exists as a dimer with two heterodimeric catalytic sites, where one monomer contributes residues for nucleotide binding and the other contributes residues for aminoglycoside binding (Sakon *et al.*, 1993; Pedersen, Benning, & Holden, 1995). Studies suggest that ANT(2'')-Ia and ANT(4')-Ia bind via similar mechanisms, and it is not uncommon for structural homology to be high despite low sequence homology. Given that ANT(2'')-Ia exists as a monomer, it is possible that different regions of the monomer contribute to the binding site for each substrate in the same way that each monomer contributes residues to the binding site of each substrate in ANT(4')-Ia.

Since ANT(4')-Ia is the only aminoglycoside nucleotidyltransferase to have been structurally characterized to date, further studies on ANT(2'')-Ia<sup>SC</sup> are needed to gain deeper insight into the mechanism of action of this family of resistance enzymes. These include NMR experiments to complete the structure of ANT(2'')-Ia<sup>SC</sup>, as well as complementary crystallographic studies. In order to understand the binding interactions and changes in conformation and protonation state upon substrate binding, complete sequential backbone assignments are needed for both ATP-bound and tobramycin-bound ANT(2'')-Ia<sup>SC</sup>. Finally, full kinetic characterization is needed on the ANT(2'')-Ia<sup>SC</sup> version that we identified, as kinetic studies have thus far only been done on the previous versions of ANT(2'')-Ia.

### **4.3 Final remarks**

Our goal is to combat resistance to this important class of antibiotics through structure-guided drug design and discovery. The more insight we gain into the mechanisms of action of resistance proteins, the better we will be able to respond to the

ongoing problems of antibiotic resistance. These preliminary studies on SpcN and ANT(2'')-Ia will hopefully set the stage for future structural studies that can aid in addressing this global issue.

## References

- Baneyx, F., & Mujacic, M. (2004). Recombinant protein folding and misfolding in *Escherichia coli*. *Nature Biotechnology*, 22(11), 1399-1408.
- Benveniste, R., & Davies, J. (1971) R-factor mediated gentamicin resistance: a new enzyme which modifies aminoglycoside antibiotics. *FEBS Letters*, 14(5), 293-296.
- Bryan, L.E., & Van Den Elzen, H.M. (1977) Effects of membrane-energy mutations and cations on streptomycin and gentamicin accumulation by bacteria: a model for entry of streptomycin and gentamicin in susceptible and resistant bacteria. *Antimicrobial agents and chemotherapy*, 12(2), 163-177.
- Busscher, G.F., Rutjes, F.P.J.T., van Delft, F.L. (2005). 2-Deoxystraptamine: Central scaffold of aminoglycoside antibiotics. *Chemical Reviews*, 105(3), 775-791.
- Cameron, F.H., Groot Obbink, D.J., Ackerman, V.P., & Hall, R.M. (1986) Nucleotide sequence of the ADD(2'') aminoglycoside adenylyltransferase determinant aadB. Evolution relationship of this region with those surrounding aadA in R538-1 and dhfrII in R388. *Nucleic Acid Research*, 14(21), 8625-8635.
- Carter, A. P., Clemons, W. M., Brodersen, D. E., Morgan-Warren, R. J., Wimberly, B. T., & Ramakrishnan, V. (2000). Functional insights from the structure of the 30S ribosomal subunit and its interactions with antibiotics. *Nature Medicine*, 407, 340-348.
- Clardy, J., Fischbach, M. A., & Currie, C. R. (2009). The natural history of antibiotics. *Current Biology*, 19(11), R437-R441.
- Daigle, D., McKay, G., Thompson, P., & Davies, J., & Davies, D. (2010). Origins and evolution of antibiotic resistance. *Microbiology and Molecular Biology Reviews*, 74(3), 417-433.
- Davis, BD. (1988). The lethal action of aminoglycosides. *Journal of Antimicrobial Chemotherapy*, 22, 1-3.

- Delaglio, F., Grzesiek, S., Vuister, G.W., Zhu, G., Pfeifer, J., & Bax, A. (1995) NMR-Pipe: a multidimensional spectral processing system based on UNIX pipes. *Journal of Biomolecular NMR*, 6(3), 277–293.
- Dyda, F., Klein, D. C., & Hickman, A. B. (2000). GCN5-related *N*-acetyltransferases: A Structural Overview. *Annual Review of Biophysics and Biomolecular Structure*, 29(1), 81-103.
- Ekman, D.R., DiGiammarino, E.L., Wright, E., Witter, E.D., & Serpersu, E.H. (2001) Cloning, overexpression, and purification of aminoglycoside antibiotic nucleotidyltransferase (2'')-Ia: conformational studies with bound substrates. *Biochemistry*, 40, 7017-7024.
- Fong, D. H., Lemke, C. T., Hwang, J., Xiong, B., & Berghuis, A. M. (2010). Structure of the antibiotic resistance factor spectinomycin phosphotransferase from *Legionella pneumophila*. *Journal of Biological Chemistry*, 285(13), 9545-9555.
- Fourmy, D., Recht, M. I., Blanchard, S. C., & Puglisi, J. D. (1996). Structure of the A site of *Escherichia coli* 16S ribosomal RNA complexed with an aminoglycoside antibiotic. *Science*, 274(5291), 1367-1371.
- García-Fruitós, E., González-Montalbán, N., Morell, M., Vera, A., Ferraz, R., & Arís, S., Ventura, S., & Villaverde, A. (2005). Aggregation as Bacterial Inclusion Bodies Does Not Imply Inactivation of Enzymes and Fluorescent Proteins. *Microbial Cell Factories*, 4(27).
- Gates, C.A., & Northrop, D.B. (1988) Alternative substrates and inhibition kinetics of aminoglycosides nucleotidyltransferase 2''-I in support of a Theorell-Chance kinetic mechanism. *Biochemistry*, 27(10), 3826-3833.
- Goddard, T.D., & Kneller, D.G., SPARKY 3, University of California, San Francisco.
- Gosselin, S., Alhussaini, M., Streiff, M.B., Takabayashi, K., Palcic, M.M. (1994) A continuous spectrophotometric assay for glycosyltransferases. *Analytical Biochemistry*, 220, 92-97.
- Hancock, R.E., Farmer, S.W., Li, Z.S., Poole, K. (1991) Interaction of aminoglycosides with the outer membranes and purified lipopolysaccharide and OmpF porin of *Escherichia coli*. *Antimicrobial Agents and Chemotherapy*, 35(7), 1309-1314.

- Hollingshead, S., & Vapnek, D. (1985). Nucleotide sequence analysis of a gene encoding a streptomycin/spectinomycin adenylyltransferase. *Plasmid*, *13*(1), 17-30.
- Hon, W., McKay, G., Thomson, P. R., Sweet, R. M., Yang, D. S., Wright, G., & Berghuis, A. (1997). Structure of an enzyme required for aminoglycoside antibiotic resistance reveals homology to eukaryotic protein kinases. *Cell*, *89*(6), 887-895.
- Kelly, A.E., Ou, H.D., Withers, R., Dötsch, V. (2002) Low-conductivity buffers for high-sensitivity NMR measurements. *JACS*, *124*(40), 12013-12019.
- Kotra, L. P., Hadad, J., & Mobashery, S. (2000). Aminoglycosides: perspectives on mechanisms of action and resistance and strategies to counter resistance. *Antimicrobial Agents and Chemotherapy*, *44*(12), 3249-3256.
- Kovacs, H., Moskau, D., Spraul, M. (2005) Cryogenically cooled probes – a leap in NMR technology. *Progress in Nuclear Magnetic Resonance Spectroscopy*, *46*, 131-155.
- Levy, S.B., & Marshall, B. (2004). Antibacterial resistance worldwide: causes, challenges and responses. *Nature Medicine*, *10*(12s), S122-S129.
- Li, R., & Cheng, C. (2009) Investigation of inclusion body formation in recombinant *Escherichia coli* with a bioimaging system. *Journal of Bioscience and Bioengineering*, *107*(5), 512-515.
- Lynch, S. R., & Puglisi, J. D. (2001). Structural origins of aminoglycoside specificity for prokaryotic ribosomes. *Journal of Molecular Biology*, *306*(5), 1037-1058.
- Lutzkanova, D., Distler, J., & Altenbuchner, J. (1997). A spectinomycin resistance determinant from the spectinomycin producer *Streptomyces flavopersicus*. *Microbiology*, *143*, 2135-2143.
- MacLeod, D. L., Nelson, L. E., Shawar, R. M., Lin, B. B., Lockwood, L. G., Dirks, J. E., . . . Garber, R. L. (2000). Aminoglycoside-resistance mechanisms for cystic fibrosis *Pseudomonas aeruginosa* isolates are unchanged by long-term, intermittent, inhaled tobramycin treatment. *The Journal of Infectious Diseases*, *181*, 1180-1184.
- Malakar, P., & Venkatesh, K. V. (2012). Effect of substrate and IPTG concentrations on

- the burden to growth of *Escherichia coli* on glycerol due to the expression of Lac proteins. *Applied Microbiology and Biotechnology*, 93(6), 2543-2549.
- Mc Dermott, P.F., Walker, R.D., White, D.G. (2003). Antimicrobials: modes of actions and mechanisms of resistance. *International Journal of Toxicology*, 22(2), 135-143.
- McKay, G.A., Thompson, P.R., Wright, G.D. (1994) Broad spectrum aminoglycoside phosphotransferases type III from *Enterococcus*: overexpression, purification, and substrate specificity. *Biochemistry*, 33, 6936-6944.
- McKay, G.A., & Wright, G.D. (1995) Kinetic mechanism of aminoglycoside phosphotransferases type IIIa. Evidence for a Theorell-Chance mechanism. *Journal of Biological Chemistry*, 270(40), 24686-24692.
- Mingeot-Leclercq M.-P., Glupczynski, Y., & Tulkens, P. M. (1999). Aminoglycosides: activity and resistance. *Antimicrobial Agents and Chemotherapy*, 43(4), 727-737.
- Mossialos, E., Morel, C., Edwards, S., Berenson, J., Gemmill-Toyama, M., & Brogan, D. (2010). *Policies and Incentives for Promoting Innovation in Antibiotic Research*. World Health Organization.
- Murphy, E. (1985). Nucleotide sequence of a spectinomycin adenylyltransferase AAD(9) determinant from *Staphylococcus aureus* and its relationship to AAD(3'') (9). *Mol. Gen. Genet.*, 200(1), 33-39.
- Novagen Technical Bulletins. (2013) *pET-22b(+)* vector, TB3038 12/98, catalogue number 69774-3. Retrieved from [http://www.emdmillipore.ca/life-science-research/technical-bulletins/c\\_IMOb.s1OXkUAAAEj2xsYzMkq](http://www.emdmillipore.ca/life-science-research/technical-bulletins/c_IMOb.s1OXkUAAAEj2xsYzMkq)
- Oliver, P., Goldstein, A., Bower, R., Holper, J., & Otto, R. (1961). M-141, a new antibiotic. I. Antimicrobial properties, identity with actinospectacin, and production by *Streptomyces flavopersicus*, sp.n. *Antimicrobial Agents and Chemotherapy*, 495-502.
- Pedersen, L. C., Benning, M. M., & Holden, H. M. (1995). Structural investigation of the antibiotic and ATP-binding sites in kanamycin nucleotidyltransferase. *Biochemistry*, 34(41), 13305-13311.

- Ramirez, M. S., & Tomalsky, M. E. (2010). Aminoglycoside modifying enzymes. *Drug Resistance Updates*, 13(6), 151-171.
- Réblová K., Lankas, F., Rázga, F., Krasovska, M. V., Koča, J., & Šponer, J. (2006). Structure, dynamics, and elasticity of free 16s rRNA helix 44 studied by molecular dynamics simulations. *Biopolymers*, 82(5), 504-520.
- Recht, M. I., & Puglisi, J. D. (2001). Aminoglycoside resistance with homogeneous and heterogeneous populations of antibiotic-resistant ribosomes. *Antimicrobial Agents and Chemotherapy*, 45(9), 2414-2419.
- Sánchez de Groot, N., & Ventura, S. (2006) Effect of temperature on protein quality in bacterial inclusion bodies. *FEBS Letters*, 580, 6471-6476,
- Sakon, J., Liao, H., Kanikula, A., Benning, M., Rayment, I., & Holden, H. (1993). Molecular structure of kanamycin nucleotidyltransferase determined to 3.0-Å Resolution. *Biochemistry*, 32, 11977-11984.
- Serpensu, E.H., Özen, C., & Wright E. (2008). Studies of enzymes that cause resistance to aminoglycoside antibiotics. In W. Scott Champney (Eds.), *Methods in Molecular Medicine*, 142 (pp. 261-271). Totowa , NJ: Humana Press Inc.
- Shakya, T., & Wright, G. D. (2010). Nucleotide selectivity of antibiotic kinases. *Antimicrobial Agents and Chemotherapy*, 54(5), 1909-1913.
- Schatz, A., Bugle, E., & Waksman, S. A. (1944). Streptomycin, a substance exhibiting antibiotic activity against Gram-positive and Gram-negative bacteria. *Experimental Biology and Medicine*, 55(1), 66-69.
- Shaw, J.J., Rather, P.N., Hare, R.S., Miller, G.H. (1993). Molecular genetics of aminoglycoside resistance genes and familial relationships of the aminoglycoside-modifying enzymes. *Microbiological Reviews*, 57(1), 138-163.
- Shi, K., Caldwell, S. J., Fong, D. H., & Berghuis, A. M. (2013). Prospects for circumventing aminoglycoside kinase mediated antibiotic resistance. *Frontiers in Cellular and Infection Microbiology*, 3, 1-17.
- Shi, K., and Berghuis, A. M. (2012). Structural basis for the dual nucleotide selectivity of aminoglycoside 2"-phosphotransferase IVa provides insight on determinants of nucleotide specificity of aminoglycoside kinases. *Journal of Biological Chemistry*, 287, 13094–13102.

- Smith, A. L., & Smith, D. H. (1974). Gentamicin: adenine mononucleotide transferase: partial purification, characterization, and use in the clinical quantitation of gentamicin. *Journal of Infectious Diseases*, *129*(4), 391-401.
- Studier, F. W. (2005). Protein production by auto-induction in high-density shaking cultures. *Protein Expression and Purification*, *41*(1), 207-234.
- Suter, T. M., Viswanathan, V., & Cianciotto, N. P. (1997). Isolation of a gene encoding a novel spectinomycin phosphotransferase from *Legionella pneumophila*. *Antimicrobial Agents and Chemotherapy*, *41*(6), 1385-1388.
- Taber, H.W., Mueller, J.P., Miller, P.F., Arrow, A.S. (1987) Bacterial uptake of aminoglycoside antibiotics. *Microbiological Reviews*, *51* (4), 439-457.
- Tsai, A., Uemura, S., Johansson, M., Puglisi, E., Marshall, R., Aitken, C., . . . Puglisi, J. (2013). The impact of aminoglycosides on the dynamics of translation elongation. *Cell Reports*, *3*(2), 497-508.
- Vakulenko, S. B., & Mobashery, S. (2003). Versatility of aminoglycosides and prospects for their future. *Clinical Microbiology Reviews*, *16*(3), 430-450.
- van Hoek, A. H. A. M., Mevius, D., Guerra, B., Mullany, P., Roberts, A. P., & Aarts, H. J. M. (2011). Acquired antibiotic resistance genes: an overview. *Frontiers in Microbiology*, *2*.
- Van Pelt, J.E.. & Northrop D.B. (1984) Purification and properties of gentamicin nucleotidyltransferase from *Escherichia coli*: nucleotide specificity, pH optimum, and the separation of two electrophoretic variants. *Archives of Biochemistry and Biophysics*, *230*(1), 250-263.
- Van Pelt, J.E., Iyengar, R., & Frey, P.A. (1986) Gentamicin nucleotidyltransferase. *Journal of Biological Chemistry*, *261*(34), 15995-15999.
- Villaverde, A., & Carrió, M.M. (2003) Protein aggregation in recombinant bacteria: biological role of inclusion bodies. *Biotechnology Letters*, *25*, 1385-1395.
- Vuillemin, P. (1889). Antibiose et symbiose. *Association française pour l'Avancement des Sciences*, *2*, 525-542.
- Waksman SA (1944) Antibiotic substances, production by microorganisms - nature and mode of action. *American Journal of Public Health Nations Health*, *34*(4), 358–364.

- Waksman, S.A. (1947). What is an antibiotic or an antibiotic Substance? *Mycological Society of America*, 39(5), 565-569.
- Walls, D., & Loughran, S. T. (2011) Tagging recombinant proteins to enhance solubility and aid purification. *Methods in Molecular Biology, Protein Chromatography: Methods and Protocols*, 681, 151-175.
- Waugh, D.S. (2011) An overview of enzymatic reagents for the removal of affinity tags. *Protein Expression and Purification*, 80(2), 283-293.
- Willis, B., & Arya, D. P. (2006). An Expanding view of aminoglycoside-nucleic acid recognition. *Advances in Carbohydrate Chemistry and Biochemistry*, 60, 251-302.
- Witte, W. (1998). Biomedecine: Medical consequences of antibiotic use in agriculture. *Science*, 279(5353), 996-997.
- Wright, D., & Berghuis, A.M. (2000). Resistance to aminoglycoside antibiotics: function meets structure. In A. Van Broekhoven, F. Shapiro, & J. Anné (Eds.), *Novel Frontiers in the Production of Compounds for Biomedical Use* (pp. 85-98). Dordrecht, the Netherlands: Lkuwer Academic Publishers.
- Wright, E. & Serpersu, E.H. (2004) Isolation of aminoglycoside nucleotidyltransferase(2'')-Ia from inclusion bodies as active, monomeric enzyme. *Protein Expression and Purification*, 35, 373-380.
- Wright, E., & Serpersu, E.H. (2005) Enzyme-substrate interactions with an antibiotic resistance enzyme: aminoglycoside nucleotidyltransferase(2'')-Ia characterized by kinetic and thermodynamic methods. *Biochemistry*, 44, 11581-11591.
- Wright, E., & Serpersu, E.H. (2006) Molecular determinants of affinity for aminoglycoside binding to the aminoglycoside nucleotidyltransferase(2'')-Ia. *Biochemistry*, 45, 10243-10250.
- Wright, E., & Serpersu, E.H. (2011) Effects of proton linkage on thermodynamic properties of enzyme-antibiotic complexes of the aminoglycoside nucleotidyltransferase(2'')-Ia. *Journal of Thermodynamics and Catalysis*, 2, 107.
- Wright, G. (1998). Aminoglycoside antibiotic phosphotransferases are also serine protein kinases. *Chemistry and Biology*, 6, 11-18.

- Wright, G. D., & Thomson, P. R. (1999). Aminoglycoside phosphotransferases: proteins, structure and mechanism. *Frontiers in Bioscience*, *4*, d9-21.
- Yu, H. (1999) Extending the size limit of protein nuclear magnetic resonance. *PNAS*, *96*(2), 332-334.
- Zheng, L., Baumann, U., Reymond., JL. (2004) An efficient one-step site directed and site-saturation mutagenesis protocol. *Nucleic Acid Research*, *32*(14), e115.

## Appendix

### Nuclear Magnetic Resonance Peak Assignments for ANT(2'')-Ia<sup>SC</sup>

**Table A-1 NMR assignments for ANT(2'')-Ia<sup>SC</sup>**

residue	amino acid	<sup>15</sup> N	<sup>1</sup> H	<sup>13</sup> C $\alpha$	<sup>13</sup> C $\beta$
1	met				
2	asp				
3	thr	114.888	8.3	59.492	66.637
4	thr	118.01	8.234	62.62	66.399
5	gln	120.354	8.465	57.527	26.361
6	val	117.79	7.606	64.277	28.569
7	thr	114.338	7.668	63.467	65.809
8	leu	121.98	7.572	55.379	38.56
9	ile	119.457	8.044	63.96	34.82
10	his	116.415	8.143	56.433	28.504
11	lys	118.599	7.137	55.755	29.625
12	ile	121.569	7.673	62.998	35.591
13	leu	119.717	7.334	54.868	37.668
14	ala	121.252	8.132	52.542	15.354
15	ala	120.743	7.47	51.724	15.877
16	ala	122.934	8.401	52.757	14.89
17	asp	121.303	8.789	54.73	37.07
18	glu	119.438	7.412	56.207	26.911
19	arg	116.087	6.957	52.039	27.375
20	asn	118.072	7.918	51.395	34.601
21	leu	122.454	8.07	48.318	41.614
22	pro				
23	leu	114.727	6.147	49.951	44.468
24	trp	120.38	8.597	55.437	29.979

residue	amino acid	<sup>15</sup> N	<sup>1</sup> H	<sup>13</sup> C $\alpha$	<sup>13</sup> C $\beta$
25	ile	123.386	8.404	57.285	34.598
26	gly	104.988	8.928		
27	gly	107.742	8.677		
28	gly	110.524	8.535	44.949	
29	trp				
30	ala	122.184	7.124	52.173	15.754
31	ile	118.591	7.308	62.515	35.598
32	asp	117.658	8.08	54.849	37.825
33	ala	122.893	8.858	51.283	16.301
34	arg	120.037	8.335	57.57	
35	leu	117.994	8.111	52.924	40.041
36	gly	109.149	8.044	43.384	
37	arg	117.416	7.9	51.812	29.999
38	val	120.259	8.109	59.411	29.826
39	thr	120.001	8.698	64.087	66.073
40	arg	118.024	8.621	56.263	28.566
41	lys	120.525	8.148		30.67
42	his				
43	asp				
44	asp				
45	ile				
46	asp	128.212	8.111	50.441	37.891
47	leu	123.036	8.734	50.439	44.146
48	thr	121.146	9.456	58.056	66.951
49	phe	123.12	8.145	49.872	40.38
50	pro				
51	gly	116.949	9.272	44.835	
52	glu	123.214	10.467	54.395	24.943

residue	amino acid	<sup>15</sup> N	<sup>1</sup> H	<sup>13</sup> C $\alpha$	<sup>13</sup> C $\beta$
53	arg	121.511	8.229	52.472	28.13
54	arg	118.205	7.735	53.088	30.03
55	gly	126.403	8.477		
56	glu	118	8.602		28.311
57	lys	118.862	6.903	54.329	38.219
58	glu	118.678	8.214	58.173	26.247
59	ala	119.3	7.496	52.268	14.993
60	ile	121.196	7.284	63.04	35.645
61	val	118.85	7.816	64.731	28.181
62	glu	117.717	7.963	56.454	26.812
63	met				
64	leu	118.235	7.416	51.889	38.883
65	gly	106.7	7.8	42.417	
66	gly	108.723	8.291	42.111	
67	arg	113.503	8.316	51.404	30.455
68	val	123.724	8.796	61.765	28.762
69	met	128.44	9.282	53.489	31.946
70	glu	116.821	7.522	53.207	30.46
71	glu	124.195	8.634	53.211	27.41
72	leu	125.474	8.093	50.44	40.332
73	asp	120.638	8.346	54.357	37.293
74	tyr				
75	gly	108.775	7.844	41.588	
76	phe	116.246	8.841	53.983	37.617
77	leu	118.753	8.711	49.789	42.053
78	ala	126.837	9.495	47.123	20.671
79	glu	119.298	8.501	51.244	30.855
80	ile	122.627	8.262	59.369	37.337

residue	amino acid	<sup>15</sup> N	<sup>1</sup> H	<sup>13</sup> C $\alpha$	<sup>13</sup> C $\beta$
81	gly	119.936	9.17	44.526	
82	asp	123.666	8.769	52.013	38.211
83	glu				
84	leu				
85	ley				
86	asp	124.879	8.718		38.445
87	cys	120.149	7.52	55.393	29.069
88	glu	122.264	8.586	56.263	32.636
89	pro				
90	ala	120.985	7.806	46.833	20.709
91	trp	118.286	8.187	52.197	29.851
92	trp	127.978	9.982	55.813	26.645
93	ala	133.896	8.057	48.714	15.797
94	asp	118.118	7.623	54.293	37.737
95	glu	114.881	7.927	52.9	27.486
96	ala	120.525	6.089	48.577	19.59
97	tyr	118.723	8.744	57.711	35.94
98	glu	115.335	8.338	51.214	30.49
99	ile	127.808	7.534	59.494	36.736
100	ala	131.944	9.109	51.702	15.87
101	glu	115.233	8.558	55.438	24.991
102	ala	121.577	7.375	47.083	15.062
103	pro				
104	gln	122.415	7.945	54.81	25.722
105	gly	115.548	10.227	41.532	
106	ser	115.825	8.584	59.015	61.704
107	cys				
108	pro				

residue	amino acid	<sup>15</sup> N	<sup>1</sup> H	<sup>13</sup> C $\alpha$	<sup>13</sup> C $\beta$
109	glu	124.116	8.666	55.917	27.208
110	ala	119.172	7.936	48.865	16.836
111	ala	123.393	8.366	49.112	14.439
112	glu	122.108	7.096	53.588	28.539
113	gly	105.687	8.03	40.81	
114	val	121.168	8.581	58.589	33.032
115	ile	123.596	8.304	57.971	38.641
116	ala	136.587	9.864	50.018	15.717
117	gly	103.557	8.133	42.52	
118	arg	123.139	7.554	49.615	30.01
119	pro				
120	val	116.029	8.288	55.793	32.417
121	arg	122.919	8.338	54.266	26.967
122	cys	117.413	9.211	52.522	29.206
123	asn	120.36	8.516	52.541	37.803
124	ser	116.277	7.354	54.39	61.752
125	trp	118.846	8.689	57.756	28.665
126	glu	116.143	9.8	58.744	25.273
127	ala	121.204	7.924	52.483	15.419
128	ile	121.072	8.083	61.941	36.481
129	ile	120.369	8.383	62.419	35.489
130	trp				
131	asp				
132	tyr	115.586	7.915	49.375	39.101
133	phe	118.231	8.319	58.636	37.661
134	tyr	122.633	9		
135	tyr				
136	ala				

residue	amino acid	<sup>15</sup> N	<sup>1</sup> H	<sup>13</sup> C $\alpha$	<sup>13</sup> C $\beta$
137	asp				
138	glu				
139	val				
140	pro				
141	pro				
142	val	112.746	7.171	28.238	61.116
143	asp	119.853	8.188	51.198	39.313
144	trp	123.524	7.623	52.059	26.52
145	pro				
146	thr				
147	lys				
148	his				
149	ile	121.609	8.526	63.125	35.564
150	glu	118.163	8.268	56.644	26.803
151	ser	116.52	7.888	61.064	
152	tyr				
153	arg				
154	leu				
155	ala	123.248	8.271	52.297	15.067
156	cys	115.031	8.144	61.091	23.916
157	thr	115.713	8.127	63.06	66.149
158	ser	117.476	7.152	59.287	
159	leu	120.555	7.156	53.812	40.156
160	gly	107.168	7.388	41.036	
161	ala	125.042	8.309	53.082	15.96
162	glu	117.773	8.719	57.274	26.02
163	lys	119.431	7.762	56.356	29.756
164	val	120.35	8.035	65.098	28.907

residue	amino acid	$^{15}\text{N}$	$^1\text{H}$	$^{13}\text{C}\alpha$	$^{13}\text{C}\beta$
165	glu	118.082	7.794	56.287	25.954
166	val	121.452	7.487	64.011	29.378
167	leu	122.405	8.025	55.172	39.949
168	arg	121.502	9.105	56.521	27.047
169	ala	121.078	7.861	52.163	14.977
170	ala	122.682	7.906	52.257	14.923
171	phe	123.238	8.78	59.515	36.566
172	arg	118.006	8.156	55.151	29.893
173	ser	113.103	7.622	57.006	60.636
174	arg	121.021	7.209	54.026	27.294
175	tyr	119.631	7.836	54.841	35.117
176	ala	124.981	7.946	50.782	16.064
177	ala	121.87	7.915	49.925	16.459
178	leu	120.414	7.94	52.323	39.72
179	glu	120.295	7.986	53.596	27.776
180	his				
181	his				
182	his				
183	his				
184	his				
185	his				